

Attention-Situation Awareness (A-SA) Model

Chris Wickens, Jason McCarley, and Lisa Thomas
University of Illinois at Urbana Champaign
Urbana, Illinois

Wickens, C., McCarley, J. and Thomas, L. (2003). Attention-Situation Awareness (A-SA) Model. In D.C. Foyle, A. Goodman & B.L. Hooey (Eds.), *Proceedings of the 2003 Conference on Human Performance Modeling of Approach and Landing with Augmented Displays*, (NASA/CP-2003-212267), 189-225. Moffett Field, CA: NASA.

This page intentionally left blank.

A. Description of Modeling Effort

A1. Foundation of the model.

The underlying theoretical structure of the Attention-Situation Awareness (A-SA) model is contained in two modules, one governing the allocation of attention to events and channels in the environment, and the second drawing an inference or understanding of the current and future state of the aircraft within that environment. The first module corresponds roughly to Endsley's (1995) Stage 1 situation awareness, the second corresponds to her Stages 2 and 3. In dynamic systems, there is a fuzzy boundary between Stage 2 (understanding) and Stage 3 (prediction) because the understanding of the present usually has direct implications for the future, and both are equally relevant for the task.

The elements underlying the attention module are contained in the **SEEV** model of attention allocation, developed by Wickens, Helleberg, Goh, Xu, and Horrey (2001; Wickens, Goh, Horrey, Helleberg, & Talleur, 2003), and are shown schematically in Figure 1 (McCarley, Wickens, Goh, & Horrey, 2002). These elements indicate that the allocation of attention in dynamic environments is driven by bottom up attention capture of **salient** events, is inhibited by the **effort** required to move attention (as well as the effort imposed by concurrent cognitive activity), and is also driven by the **expectancy** of seeing **valuable** events at certain locations in the environment. The first letter of each of the four boldfaced terms, defines the SEEV model.

In Wickens and McCarley (2001), we applied a version of this attention model, coupled with a version of an inference model based on the belief updating model of Hogarth and Einhorn (1992), to develop a version of the A-SA model that could be applied to predicting errors in taxiway navigation, as shown in Figure 2. In this modeling effort, greatest emphasis was placed on carefully defining parameters of salience of events, the effort (workload) of ongoing activity and dividing attention between multiple events, and on the **relevance** of events. Relevance was assumed to correspond to the value of those events to the pilot's task of understanding, or maintaining awareness of which direction he was supposed to turn at a given taxiway intersection. This understanding was modeled by the belief updating module with memory decay, and ranged from perfect (in which case a turn was always correct) to absent, in which

SEEV MODEL

$$P(\text{Attend}) = a_{\text{Salience}} - b_{\text{Effort}} + c_{\text{Expectancy}} + d_{\text{Value (or CEV)}}$$

**“Capture”
Contrast
Onset
Eccentricity**

**Probability
Cueing**

**Concurrent
Workload**

**Scan Distance
Foveal/Eye/Head Field**

**Value of Event
Value of Task
Relevance of event
for valued task**

Optimal

$$P(\text{Attend}) = c_{\text{Expectancy}} + d_{\text{Value}} \quad (\text{if calibrated})$$

Designer:

Reduce Effort

Make Salient

Figure 1. The SEEV model.

EVENTS

E(C,V): Conspicuity, Info Value (relevance to situation of interest)

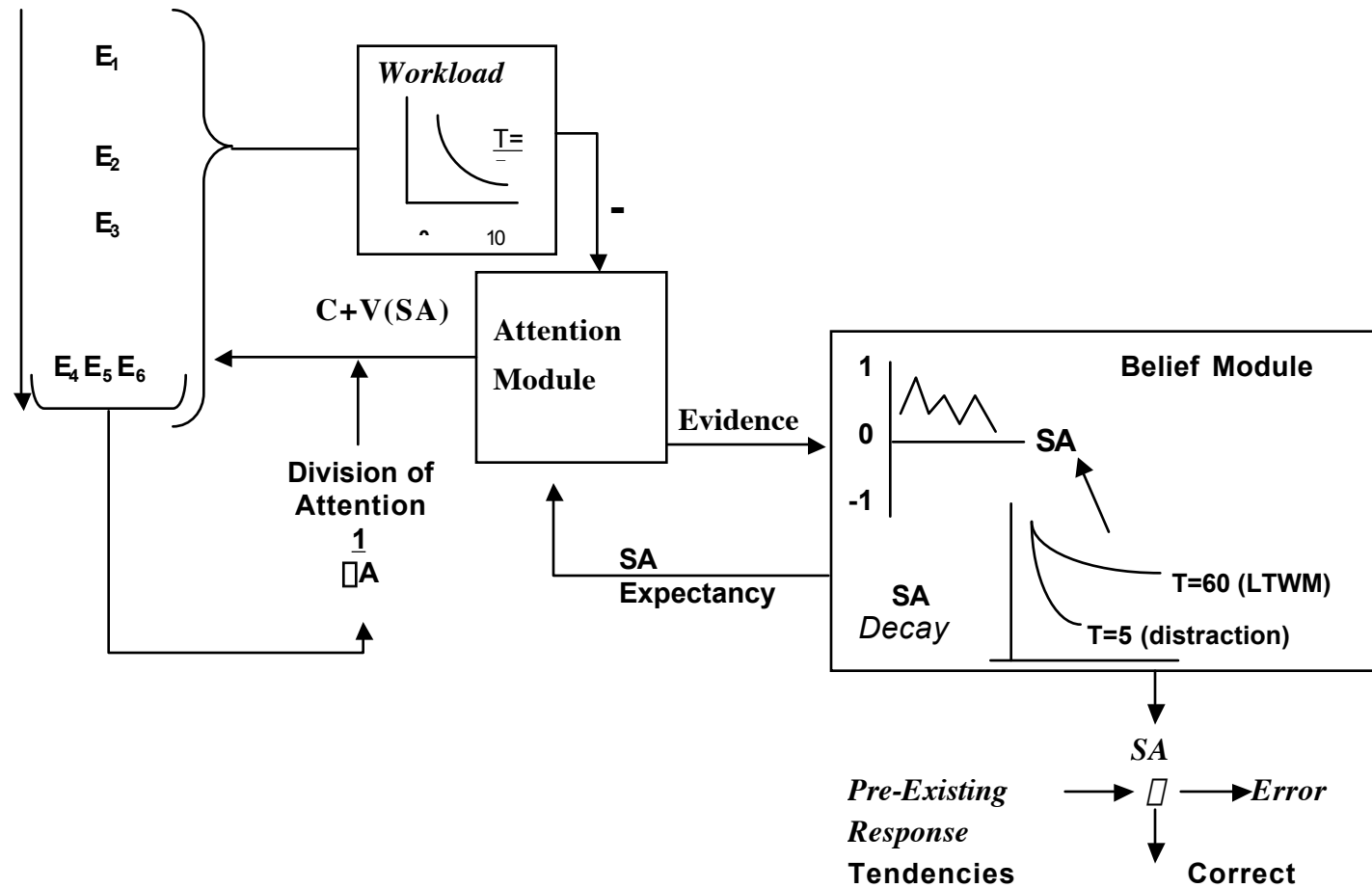


Figure 2. A-SA Model for taxi-way error prediction.

case a turn was governed by pre-existing response tendencies, which could therefore trigger a wrong turn error. We were provided by NASA with a rich set of taxiway turn errors for model validation performance data, and we were directly able to attribute these errors to a loss of situation awareness.

In the second year of the project, we were asked to apply the model to a very different sort of data, describing pilots performing simulated approaches to an airport, when supported or not supported by a synthetic vision system (SVS) display, intended by designers to support situation awareness. The NASA part-task simulation and data set supplied to us are described elsewhere in this proceedings (Goodman, Hooey, Foyle & Wilson, 2003). Several things about this new validation effort required us to modify our modeling approach from that used in the first year. First, loss-of-SA incidents were now quite scarce in the data provided by NASA. Second, we did not have available any explicit or implicit “probes” of SA (e.g., SAGAT measures; Endsley, 1995) that might also have aided data for modeling. Third, although we were provided with a full set of data records in both video and digital files, these revealed few discrete “events” that could be tied to the gain or loss of SA, in the same manner that the events from the taxiway data had been able to do. With fewer “events” it became more difficult to employ the salience component of the SEEV model, since salience serves the model only to the extent that it can be defined as a direct property of a discrete event.

To compensate for these shortcomings of the current data set, we were provided an extensive set of eye-movement data, which, in contrast to the first year taxi-data, we could now model directly as the output of our attention module. In addition, while we did not have events defined by salience, we **did** now have available channels defined by distinct locations. Following the precedence of our previous scanning model approaches, we define these channels as **Areas of Interest (AOI)**. Each AOI can be defined in terms of a (1) **transition to it**, or “**visit**” (from another AOI), a (2) **dwelt duration** on the AOI before leaving it, and a (3) **percentage dwelt time** looking at it (which is the product of the frequency of visits and the mean dwelt duration, divided by the total amount of time). While we could not thereby model the salience of events, we were able to model the **effort** of moving attention (transitioning) from one AOI to another, assuming that such effort is monotonically related to the distance between AOIs. These distances could be derived from the simulation dimensions provided to us by NASA. Furthermore, since the approach/landing task is one that has been often studied within the aviation domain, we were able to define the **value** of tasks on the well established hierarchy of **aviate > navigate**.

Following the procedures developed in Wickens, Helleberg, Goh, Xu, and Horrey (2001; Wickens et al., in press), we modeled the value of an AOI to be the value of the task served by the AOI multiplied by the relevance of that AOI to the task in question. Finally, also following similar procedures to those used in Wickens et al. (2001), we modeled the **expectancy** for information contained in an AOI, in terms of the **bandwidth** of information in that AOI (that is, the frequency with which events or changes occurred to information contained within the AOI). Thus we were able to estimate the quantitative parameters necessary to predict how frequently an AOI optimally **should** be visited, as a function of the momentary relevance and bandwidth of that AOI, and to predict how frequently it **will** be visited, given the inhibiting influence of effort (which inhibits scans over wide visual angles).

A2. General Approach to Modeling

Figure 3 provides our schematic representation of the approach to the landing used in the current SVS simulation. Importantly, each approach in the 10 scenarios that were described by NASA can be subdivided into four phases, distinguished from each other by potential changes in relevance and bandwidth (in some scenarios):

- Phase 1. Above 1000 ft. Regular “steady state” flight.
- Phase 2. 1000 ft – 850 feet. Lined up on runway (whether visible or not).
- Phase 3. 850-600 feet. Runway becomes visible as the airplane drops below the cloud ceiling in most IMC scenario landings.
- Phase 4. Below 600 feet. Runway remains hidden in low-visibility go-around scenarios.

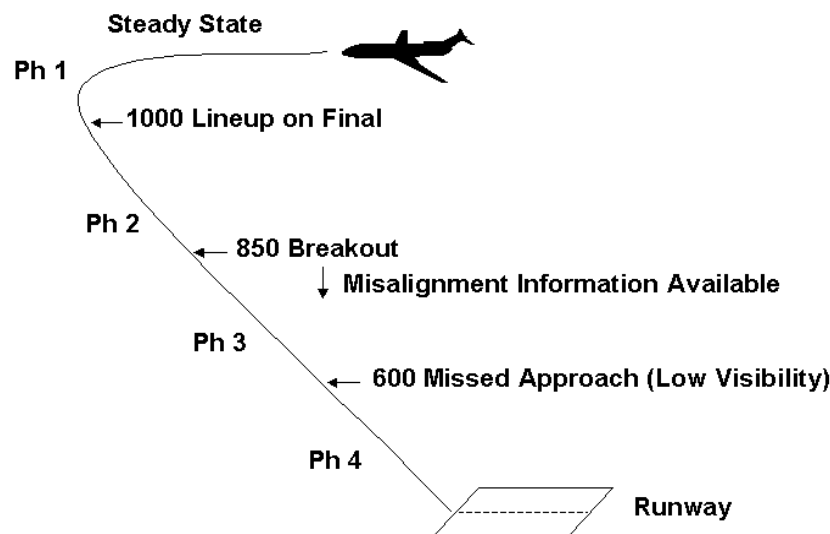


Figure 3: Schematic representation of scenario time line

Each of these phases defines a separate eye-movement data base to be analyzed. With this representation of the data, we applied four different approaches to the analysis, as shown in the 2x2 matrix of Figure 4. The figure differentiates the extent to which we are interested in the common general behavior of all pilots (left) or differences in the specific behavior of individual pilots (right), and the extent to which our modeling efforts are applied to pilot performance (top row) versus applied to visual scanning (bottom row). While the general scan data were modeled for all six scenarios (5-10) that were flown in IMC, we chose to model in detail, two landing scenarios provided by NASA, because both were characterized by some performance data, from which variability in situation awareness (between pilots) could be inferred. These were scenario 6, a baseline scenario flown in IMC, in which a mismatch between the visible runway and the ILS instrument forced a go-around below 850 feet, and scenario 10, in which the same mismatch was reflected in a misalignment between the SVS display, and the runway view.

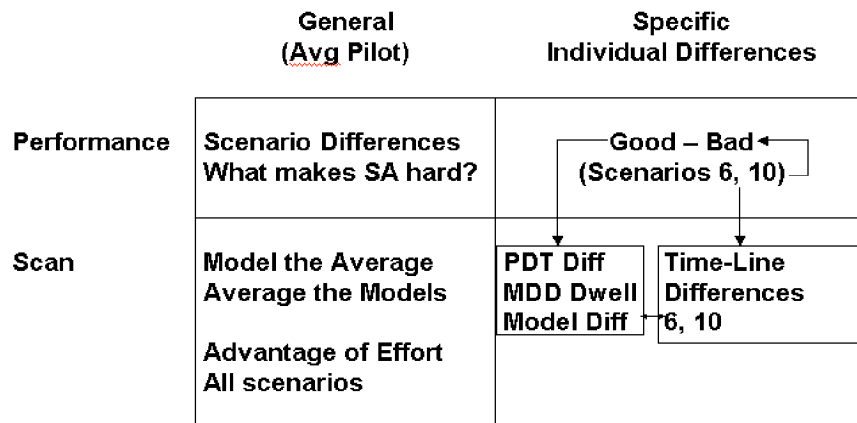


Figure 4: Different approaches to data analysis

In the upper right cell of Figure 4, the quality of situation awareness was operationally defined from performance measures by the speed with which pilots became aware of the misalignment in the two scenarios. Careful review of the video tapes and transcriptions revealed that in both scenarios, pilot 5 maintained good SA, rapidly noticing the misalignment and executing the missed approach, whereas pilots 3 and 4 either noticed this only after a considerable delay, or not at all, needing to be reminded by the confederate first officer. The distinction between the two “classes” of pilot behavior (“good” and “bad” SA) was important, allowing us to discriminate their attention allocation behavior, as we describe below

A3. Implementation of the Model

In implementing the model, we estimated the coefficients of bandwidth, relevance and task priority, as shown in Figure 5a (scenario 6) and 5b (scenario 10) both involving a missed approach. Using the same procedures applied by Wickens et al. (2001, 2003), we employed the “least integer ordinal value” heuristic, in assigning these coefficients. This is a heuristic that maintains integer values of all coefficients, and tries to keep these as low (and therefore simple) as possible, while preserving any necessary ordinal relations. As one example, the bandwidth of the instrument panel during a missed approach (climbing, accelerating, turning), is higher than during a straight in approach (compare the bandwidth parameters in Figure 5 above – straight in—and below – missed approach – the 650 ft level). The reader can also see in Figure 5a, that in IMC conditions, when the outside world (OW) is not visible, its bandwidth is assigned a value of 0. As another example, the relevance of both aviating and navigating is increased during the missed approach phase below 650 ft because of the higher criticality of both of these tasks at unusual attitudes and low to the ground.

In addition to these parameters, integer parameters for effort were assigned on the basis of the distance between displays, as extracted from the documentation provided by NASA (**Figure 2 in Goodman, Hooey, Foyle & Wilson, 2003**). Laterally adjacent displays imposed an effort value of 1, vertically separated displays, an effort value of 2, and the presence of an intervening displays also imposed an effort value of 2 for scans between the two flanking displays.

S10		Above 1000 ft	1000-800	800-650	Below 650
Parameter					
Bandwidth (B)	IP	3	3	3	5
	OW	0	0	2	3
	ND	1	1	1	1
	SVS	2	2	2	3
Relevance (R)	IP (av)	2	2	2	3
	IP (nav)	1	1	1	2
	OW (av)	0	0	1	0.5
	OW (nav)	0	0	2	1.5
	ND (av)	0	0	0	0
	ND (nav)	2	1	1	2
	SVS (av)	1	1	2.5	0.5
	SVS (nav)	1	2	2	1.5
Priority (V)	Aviate	2	2	2	4
	Navigate	1	2	2	3

Figure 5b: Coefficient Values for Scenario 10

Our model calculated the “attractiveness” of an AOI as a direct function of the product of its bandwidth and relevance (the latter, modulated by the value of the task to which AOI it was relevant). To this product was added three *minus* the effort required to reach that channel from the currently-attended AOI. This ensured that an increase in the effort needed to reach an AOI would decrease the attentional weight of that AOI. Thus, when effort needed to reach an AOI was minimal (a value of 0) , attentional weight of the object was increased by 3. When the effort needed to reach an AOI was maximal (a value of 3), attentional weight of the object was not increased relative to the value established based on bandwidth and relevance. The probability with which attention shifted to a given AOI was then calculated by dividing the attentional weight of that AOI by the summed attentional weights of all AOIs. The model thus predicted the movement of attention from one AOI to another.

We developed two versions of the model. In version 1, upon attention landing on an AOI, the relevance of that AOI became zero (reflecting the acquisition of needed dynamic information from that AOI), and the attentional weights of the remaining AOIs were recalculated so that the next gaze could occur. In version 2, the relevance would remain the same after a fixation, and the model would either move to another AOI **or** remain on the AOI with a probability that was related to the relative attentional weights of all available AOIs (including that of the momentary fixation). In this way, the eye could remain for a **long dwell** on a particular AOI, of high relevance.

Thus, for each phase of flight (characterized by its unique set of values as shown for two of the scenarios in Figure 5), the model generated an NxN transition probability table, where N was set equal to the number of “active” AOIs. For example, as can be seen in Figure 5a, in scenario 6 (baseline), N was equal to 3 (Instrument panel, IP, navigational display ND, and Outside World, OW), whereas in Figure 5b (SVS) N was equal to 4, since the SVS display itself defined a now-active AOI. Table 1 presents the active AOIs for scenarios 5 through 10, in each of the four phases. (Fixations on the MCP or other areas were sufficiently rare that these were not included in our modeling efforts).

The cell values of a transition table from model version 1 defined the predicted probability of **transitioning** from one AOI to another. The row (or column) values within the table provided the predicted **number of visits**, or “popularity” of an AOI. In version 1, if we assumed that the number of visits was correlated with the length of each visit, we could label this as a prediction of the percentage dwell time (PDT) on each AOI. In model version 2, we were able to predict the PDT directly by summing the total time of dwells on each AOI, and dividing by total trial time. In either case, we were then able to correlate these two model-derived measures (transitions within each cell and PDT), with the actual scanning behavior extracted from the eye movement records of each pilot, in each of the 4 phases of each scenario, to provide measures of model validation. Finally, it was possible to compute such correlations in either of two ways: (1) compute the correlation of each pilot individually, and average the correlation, (2) compute the average scanning data across the 3 pilots, and correlate these averaged data with the model prediction (only two pilots provided scanning data for scenario 6).

Table 1. Active AOI's (✓) for each scenario and phase.

<div style="text-align: center;"> <div style="display: inline-block; width: 100%; border-bottom: 1px solid black; position: relative;"> → </div> Phase </div>					
Scenario	AOI	1	2	3	4
5	OW				
	IP	✓	✓	✓	✓
	ND	✓	✓	✓	✓
	SV				
6	OW			✓	✓
	IP	✓	✓	✓	✓
	ND	✓	✓	✓	✓
	SV				
7	OW			✓	✓
	IP	✓	✓	✓	✓
	ND	✓	✓	✓	✓
	SV	✓	✓	✓	✓
8	OW			✓	✓
	IP	✓	✓	✓	✓
	ND	✓	✓	✓	✓
	SV	✓	✓	✓	✓
9	OW			✓	✓
	IP	✓	✓	✓	✓
	ND	✓	✓	✓	✓
	SV	✓	✓	✓	✓
10	OW			✓	✓
	IP	✓	✓	✓	✓
	ND	✓	✓	✓	✓
	SV	✓	✓	✓	✓

B. Findings

B1. Modeling the average pilot.

Using model version 1, we computed the model fitting correlations based on transitions, and based on 4 different versions of the PDT predictions. These four versions involved the presence or absence of the **effort** parameter, and involved either correlating model predictions with the average scanning behavior of the 3 pilots, or averaging the correlation values $\{r\}$ across the three pilots. From this exercise with model version 1, we drew the following three conclusions:

1. Methodologically, the correlation with the average scan data (average $r = 0.79$) is greater than the average of the pilot correlations ($r = 0.60$).
2. The correlations (model fits) with the PDT (average = 0.60) are generally higher than those with the Transitions (average = 0.42). The reason for the decrease in the latter values is, presumably, that the model predicts symmetric transition probabilities between AOIs (e.g., $P(OW \rightarrow IP) = P(IP \rightarrow OW)$), and the data may show asymmetries of direction.
3. The inclusion of the Effort parameter offers no benefit to model fitting, and in fact, in some cases, actually reduces the fit. We conclude from this, that pilots were not inhibited from making longer scans, if there was valuable and high-bandwidth information to be obtained at the more distant AOI. Such a conclusion was also consistent with one drawn by Wickens et al. (2001). However a decision was made to retain the effort parameter in our subsequent modeling efforts because of its cognitive plausibility, and because it could be valuable in modeling differences between pilots.

We subsequently decided to proceed by modeling all individual scenarios with model version 2 (predicting percentage dwell time), as this version generally provided higher model fits across the scenarios and phases; and in particular, those phases in which more than 2 AOIs were “active” (see Table 1). Furthermore, such a model did produce dwell time differences that accounted, partially, for the different percentage dwell durations. Appendix A shows the scatter-plots between predicted and obtained PDT, on each page representing the four approach phases for each pilot. Data points for the four AOIs are labeled in the figure, whether these are “active” or not. Each scatter plot generated a correlation, and Table 2 presents the resulting correlations. From the table one can again discern the generally higher correlations for the model of the average pilot, than for the average of individual pilots. More important however, are the following two observations.

4. The average subject model fits, along with the model fits of individual pilots are all generally good, with positive correlations generally in the .60 to .80 range, although there are some exceptions. In particular, scenario 6 shows lower correlations. One possibility is that scenario 6 had only two pilots contributing eye movement data, and one of these (pilot 3) had very poor individual fits on all three phases (see top line of Table 2, Scenario 6). This point will be important below. There does not appear to be any common trend that would discriminate higher correlations from lower ones (i.e., later versus earlier phases, or SVS versus non-SVS scenarios).

Table 2. Correlations between model version 2 (with effort) and obtained data on percentage dwell time. (Eye movement data were missing for subject 4 scenario 6.)

						Description of Scenario
Scen05						
	TOTAL DWELL TIME					
		Phase 1	Phase 2	Phase 3	Phase 4	
	s03	0.738	0.841	0.513	0.776	Missed approach
	s04	0.696	0.721	0.768	0.776	(Low ceiling)
	s05	0.728	0.900	0.655	0.591	Baseline display
	Average Subject	0.756	0.839	0.466	0.813	
	Average of subjects	0.721	0.821	0.645	0.714	
Scen06						
	TOTAL DWELL TIME					
		Phase 1	Phase 2	Phase 3	Phase 4	
	s03	0.119	-0.086	-0.174	0.207	Missed approach
	s04					Terrain (ILS)
	s05	0.611	0.703	0.985		Mismatch
	Average Subject	0.347	0.290	0.457	0.207	Baseline display
	Average of subjects	0.365	0.309	0.406	0.207	
Scen07						
	TOTAL DWELL TIME					
		Phase 1	Phase 2	Phase 3	Phase 4	
	s03	0.747	0.463	0.694	0.813	Normal landing
	s04	0.310	0.960	0.903	0.978	SVS display
	s05	0.640	0.732	-0.302	0.081	
	Average Subject	0.664	0.895	0.724	0.921	
	Average of subjects	0.566	0.718	0.431	0.624	
Scen08						
	TOTAL DWELL TIME					
		Phase 1	Phase 2	Phase 3	Phase 4	
	s03	0.819	0.747	0.194	0.325	Late runway sidestep
	s04	0.652	0.850	0.677	0.409	SVS display
	s05	0.581	0.763	-0.383	0.243	
	Average Subject	0.643	0.645	0.692	0.875	
	Average of subjects	0.684	0.787	0.163	0.326	
Scen09						
	TOTAL DWELL TIME					
		Phase 1	Phase 2	Phase 3	Phase 4	
	s03	0.670	0.605	-0.121	0.346	Missed approach
	s04	0.710	0.921	0.253	0.774	(Low ceiling)
	s05	0.594	0.251	0.816	0.535	SVS display
	Average Subject	0.637	0.751	0.278	0.771	
	Average of subjects	0.658	0.593	0.316	0.552	
Scen10						
	TOTAL DWELL TIME					
		Phase 1	Phase 2	Phase 3	Phase 4	
	s03	0.638	0.858	0.276	0.103	Missed approach
	s04	0.701	0.912	0.536	0.420	(Terrain mismatch)
	s05	0.815	0.347	0.363	0.163	SVS display
	Average Subject	0.664	0.780	0.583	0.898	

5. A review of the scatter plots of the individual subject data (see Appendix) appears to reveal one consistent trend, which would account for a drop in the correlations. That is, often when the correlation is low, it is because OW scanning occurs much more frequently than predicted by the model, whereas rarely if ever is OW scanning done less than predicted. There are two possible explanations for this. First, in phases 1 and 2, the OW is invisible (IMC), and our model therefore predicts no “relevance” for either aviating or navigating tasks (see Figure 5). However it is likely that a vigilant pilot, knowing that visibility will be required for landing, will occasionally glance to the OW to assess whether anything is visible. Second, in phases 3 and 4, when the OW is visible (in all but scenarios 5 and 9, which were missed approaches because of the low clouds). The increased OW scan could reflect the fact that the OW was used both for aviating (the true horizon, rather than the IP or SVS horizon) as well as navigating (the true runway, rather than the SVS runway), thereby increasing the “relevance” coefficients (for the OW for aviating) from the model values that we assumed and assigned in Figure 5.

B2. Modeling individual pilot differences.

As we discussed in section A2, there appeared to be differences between pilots in their awareness of the runway offsets in scenarios 6 and 10. Hence we also asked if differences in the model fits might have accounted for the distinct differences between pilot 5 on the one hand, who appeared on the basis of the offset-noticing performance data, to have “good SA”, and pilots 3 and 4, who did not because they either failed to notice, or noticed very late, the misalignments. The data provided only modest support for this difference. For scenario 6, phase 2, which would characterize the scan pattern just prior to the information regarding the misalignment becoming available, the model fit for pilot 5 ($r = .70$) is much better than for pilot 3 ($r = -.08$). (There were no eye movement data for pilot 4.) More detailed examination of these differences revealed that pilot 5 looked at the PFD (a scan necessary to notice the misalignment), whereas pilot 3 did not look there during this phase (see Appendix).

For scenario 6, phase 3, similar findings revealed better model fits for pilot 5 ($r = .98$) than for pilot 3 ($r = -0.17$). More detailed examination of the scan records suggests that the lower model fit results because pilot 3 again fails to look at the PFD, where evidence of the misalignment is present.

Finally, for scenario 10, phase 2, the findings are far less consistent. Indeed pilot 5 appears to show a much poorer model fit than do pilots 3 and 4. The cause of the low prediction of pilot 5 for scenario 10 phase 2 appears to be scanning much longer on the SVS than the model predicts and much less on the PFD, an issue that will be addressed below. Similarly, during phase 3, when the discrepancy should be noticeable, there is again a poorer model fit for pilot 5, than for pilot 4 (although 5 is better than 3). Thus, in general, there is not a great deal in the model fitting that predicts differences in scan pattern during the critical time period (phase 3) when the discrepancy should be noticed. To seek these differences we turned to a final level of descriptive analysis of eye movements using a qualitative approach which departed from our quantitative modeling approach.

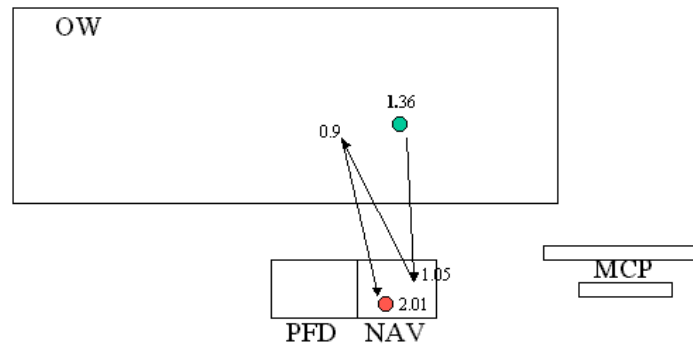
B3. Describing pilot differences in scanning behavior.

The A-SA model accounts for stable, averaged scanning data, but in its current form does not account for the micro-strategies underlying specific scans or transitions. Yet such micro-strategies appear to underlie, in particular, the difference between the one “good” SA pilot (#5) and the two other pilots (#3 & 4). These micro-strategies are illustrated in Figure 6 which shows the scan pattern and associated dwell durations for phase 3 of scenario 6 (Figure 6a, pilots 3 and 5) and of scenario 10

(Figure 6b, pilots 3, 4 and 5). This phase, (phase 3), is chosen since it is the one during which information regarding the discrepancy between the outside world and the instruments (PFD: S6 or SVS display: S10) becomes visually available. The time in the sequence of the “noticing response” – initiation of a go-around – by pilot 5 is indicated by the * in the figure. This time was extracted from the time line record of flight control parameters provided to us by NASA.

In both scenarios, pilot 5 shows two features: (1) a direct scan between the two relevant AOIs, reflecting, we infer, such a comparison necessary to notice the mismatch; (2) a long dwell (>5 seconds) on the outside world, reflecting, we infer, a careful evaluation of the information content of that AOI (runway location) with the long dwells required to notice the discrepancy. The initiation of the go-around occurs within one second after this fixation pattern is completed. Neither pilot 3 nor 4 show both of these features of the discrepancy-noticing fixation in conjunction, and in particular, neither pilot shows a long dwell on the outside world.

Pilot AOI Scanning Patterns
Scenario 6, Subject 3
800-650 ft, Dwell times ≥ 0.2 sec



Pilot AOI Scanning Patterns
Scenario 6, Subject 5
800-650 ft, Dwell times ≥ 0.2 sec

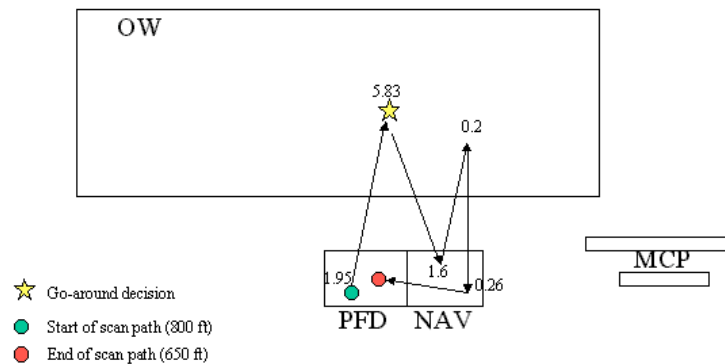
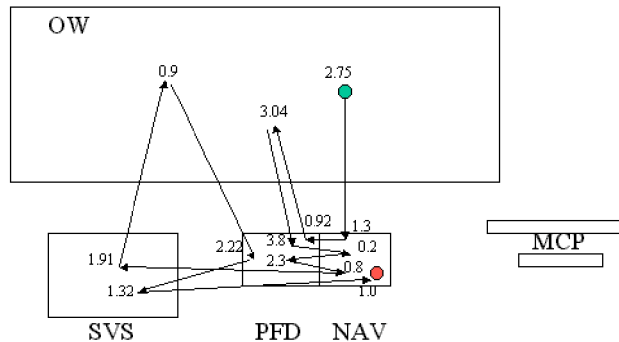
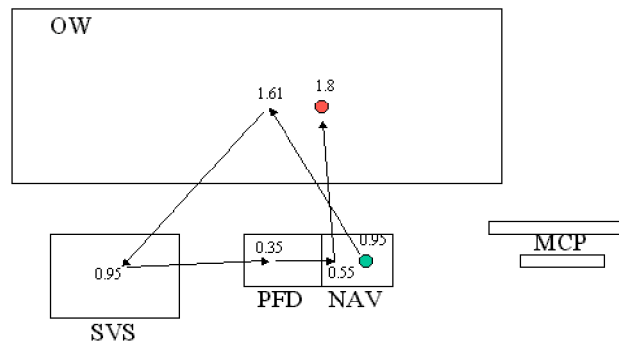


Figure 6a: Qualitative analysis of noticing runway offset, an awareness which was successful for subject 5, but not for subject 4. Scan path is Scenario 6.

Pilot AOI Scanning Patterns
Scenario 10, Subject 3
800-650 ft, Dwell times ≥ 0.2 sec



Pilot AOI Scanning Patterns
Scenario 10, Subject 4
800-650 ft, Dwell times ≥ 0.2 sec



Pilot AOI Scanning Patterns
Scenario 10, Subject 5
800-650 ft, Dwell times ≥ 0.2 sec

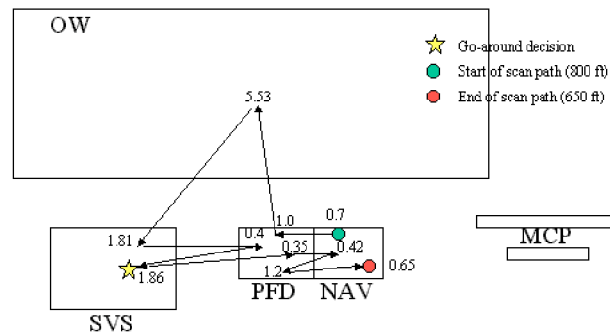


Figure 6b. Qualitative analysis of noticing runway offset, an awareness which was successful for subject 5, but not for subject 4. Scan path is scenarios 10.

C. Implications

One implication of the current modeling exercise appears to be that, in the environment modeled here, the effort of making longer scans does not appear to inhibit those scans. That is, the model fit is just as good, when driven by only bandwidth and relevance, as when effort is included. Such a conclusion is consistent with our findings in previous research (Wickens et al., 2001), that scanning of instrument rated general aviation pilots can be very effectively modeled with only expectancy and value as parameters.

A second implication is inherent in the better model fit of the “good” SA pilot (pilot 5), relative to pilot 3, a discrimination that provides some validation of the model in scenario 6.

A third implication is that the wide individual differences that appear to exist within the data provided, may be modeled as much by the dwell duration (see Figure 6), as by the particular transition. Such a distinction is one drawn by Harris and Christliff (1980), and Bellenkes, Wickens, and Kramer (1997) between short dwells, designed to confirm hypotheses, and longer dwells, designed to acquire new visual information. However the dividing line between these two forms of dwells here (around 2 seconds) is generally longer than that observed by Bellenkes et al and by Harris and Christliff (around 1 second) This discrepancy can in part, be accounted for by the fact that those investigators did not examine scanning in off-normal scenarios. It is also appropriate to note that our operational definition of “dwell duration” is not the length of a single fixation at a point location in space, but rather, refers to the duration of a repeated series of consecutive fixations within a wider AOI, before that AOI is left.

D. Lessons Learned

In terms of our modeling effort, we are learning the importance of incorporating dwell duration into our modeling. The initial step in this direction was taken with model version 2, although we have not yet exercised the model to predict the mean dwell duration.

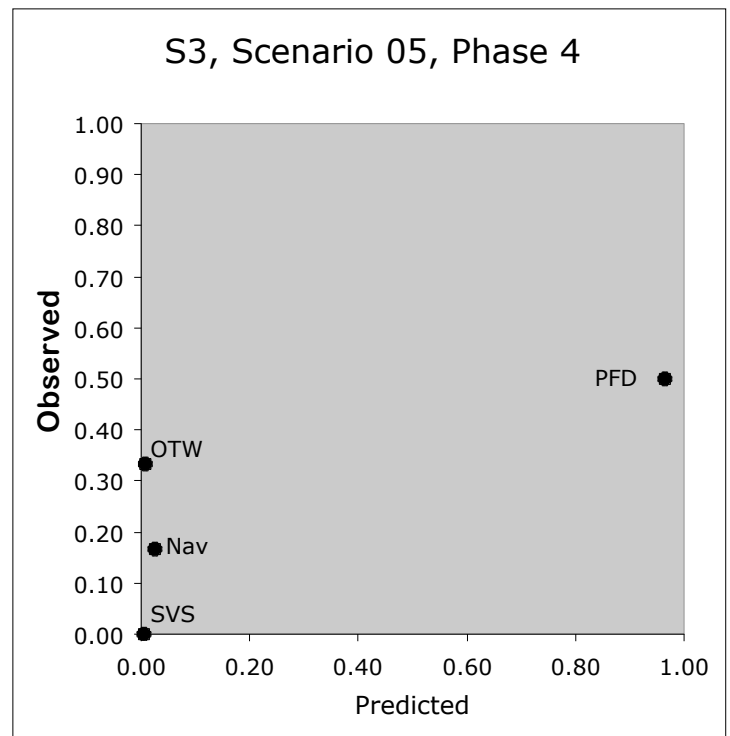
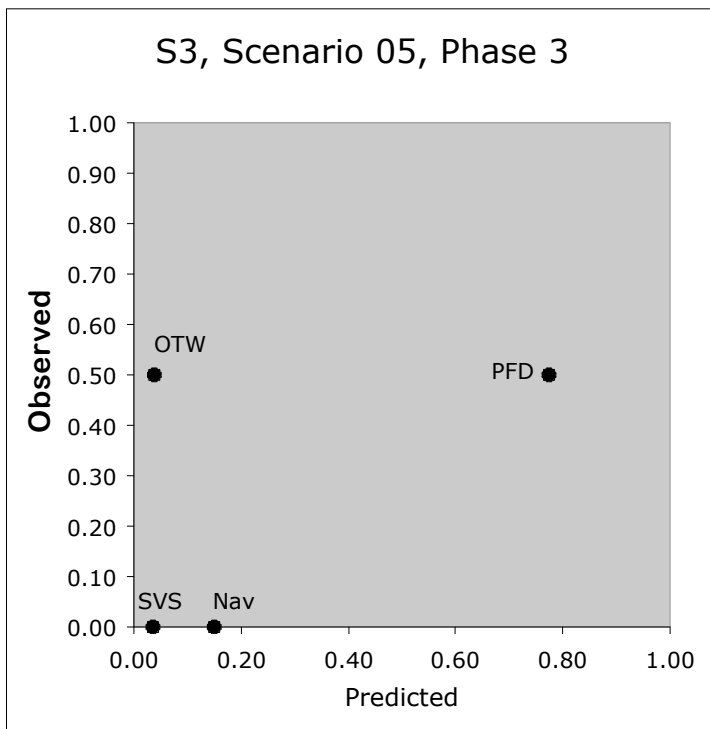
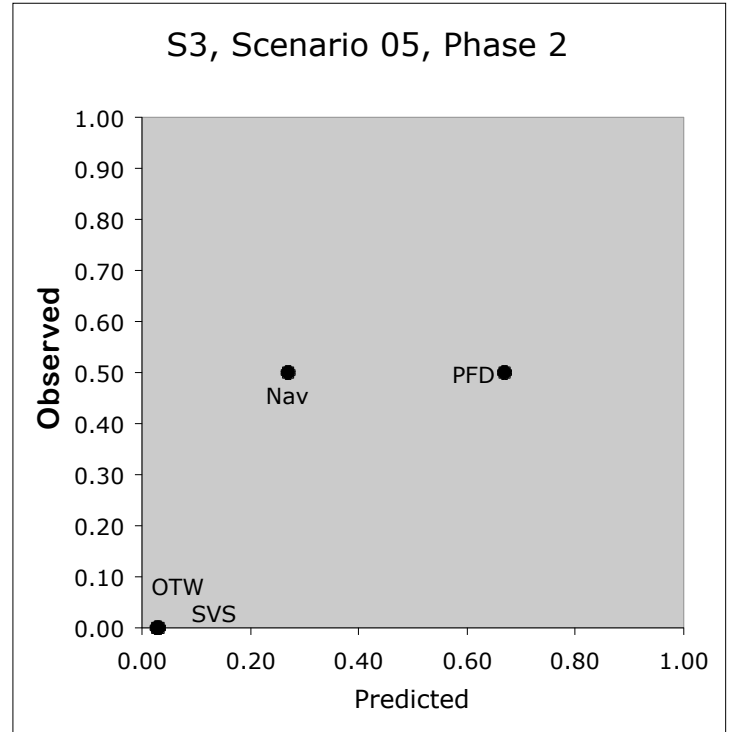
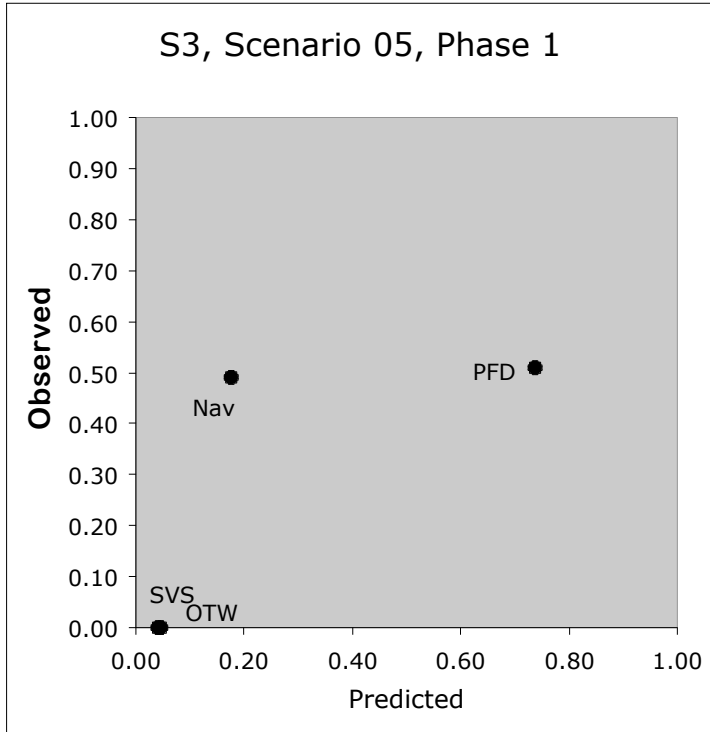
We believe that our particular modeling effort suffered from the paucity of direct “situation awareness” measures available in the current simulation, and hence a “lesson learned” might be the need to obtain explicit SA measures collected in future simulations. That is, as noted, our primary focus has been on modeling Stage 1 SA (Attention and noticing events, inferred from scanning), rather than modeling the objective of Stage 1 SA, inherent in Stages 2 and 3 (understanding and prediction). We were not able to firmly link the former to the latter, because of the paucity of data that could be used to infer the presence or absence of Stages 2 and 3 SA. Correspondingly a more robust test of the model can be achieved with data from a greater number of pilots. This would provide a wider range of responses to off-normal events, a criterion that could be used for performance based model validation. In this context we did feel fortunate that the pronounced differences between the two classes of pilots (5 vs. 3&4) emerged.

References

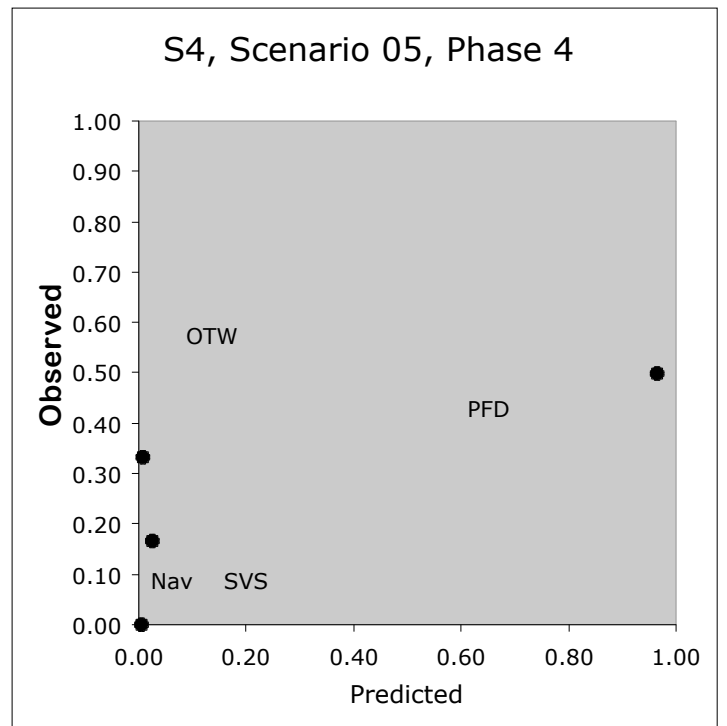
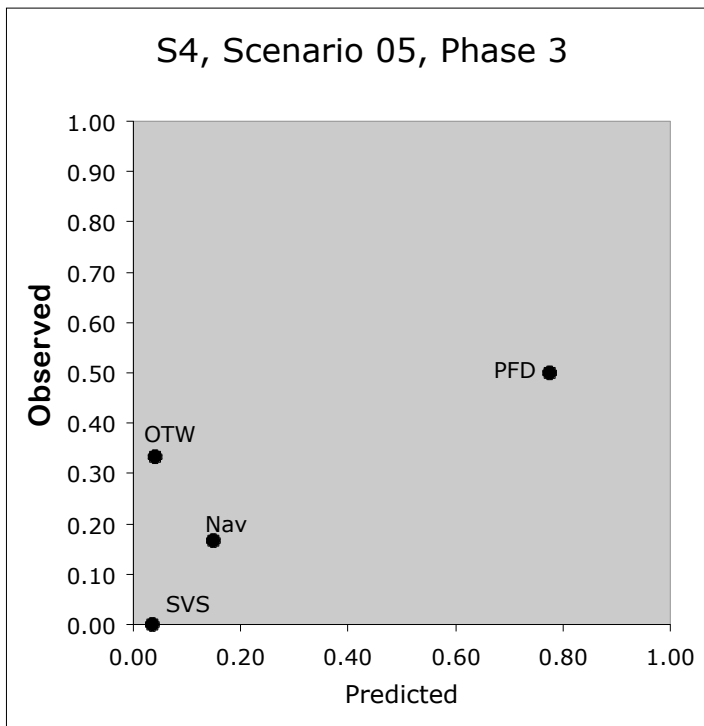
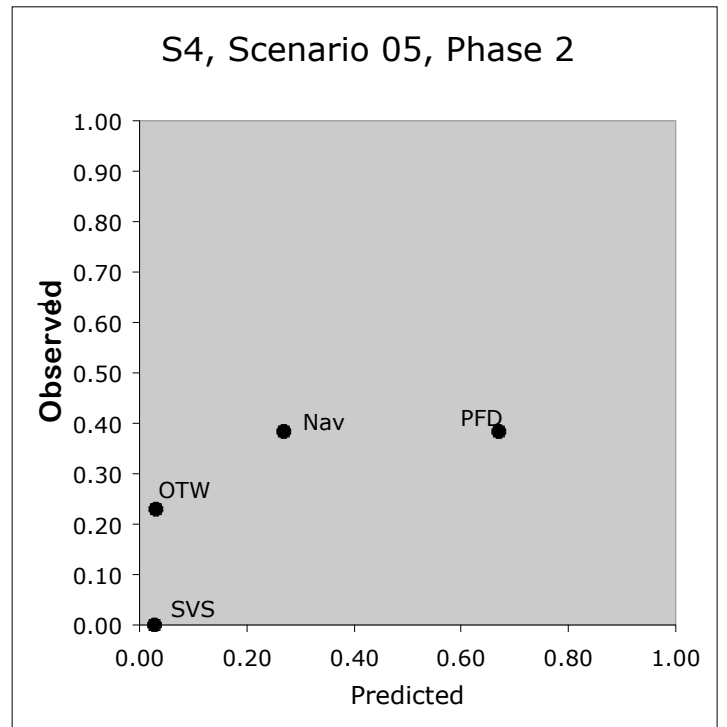
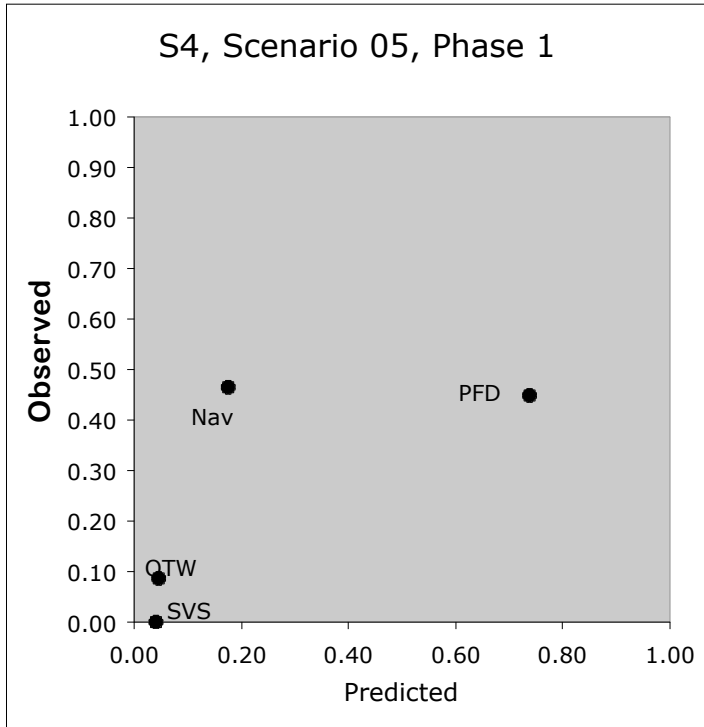
- Bellenkes, A. H., Wickens, C. D., & Kramer, A. F. (1997). Visual scanning and pilot expertise: The role of attentional flexibility and mental model development. Aviation, Space, and Environmental Medicine, 68(7), 569-579.
- Endsley, M. R. (1995). Toward a theory of situation awareness in dynamic systems. Human Factors, 37(1), 85-104.
- Goodman, A., Hooey, B.L., Foyle, D.C. and Wilson, J.R. (2003). Characterizing visual performance during approach and landing with and without a synthetic vision display: A part-task study. In Conference Proceedings of the 2003 NASA Aviation Safety Program Conference on Human Performance Modeling of Approach and Landing with Augmented Displays, (David C. Foyle, Allen Goodman & Becky L. Hooey, Eds.). NASA Conference Proceedings NASA/CP-2003-212267.
- Harris, R. L., & Christliff, D. M. (1980). What do pilots see in displays? In G. Corrick, E. Hazeltine, & R. Durst (Eds.), Proceedings of the 24th Annual Meeting of the Human Factors Society. Santa Monica, CA: Human Factors Society.
- Hogarth, R. M., & Einhorn, H. J. (1992). Order effects in belief updating: The belief-adjustment model. Cognitive Psychology, 24, 1-55.
- McCarley, J. S., Wickens, C. D., Goh, J., & Horrey, W. J. (2002). A computational model of attention/situation awareness. Proceedings of the 46th Annual Meeting of the Human Factors and Ergonomics Society. Santa Monica, CA: Human Factors and Ergonomics Society.
- Wickens, C.D., Goh, J., Horrey, W.J., Helleberg, J.H., & Talleur, D.A. (2003). Attentional models of multi-task pilot performance using advanced display technology. Human Factors, 45, #3, 360-380.
- Wickens, C. D., Helleberg, J., Goh, J., Xu, X., & Horrey, B. (2001). Pilot task management: testing an attentional expected value model of visual scanning (ARL-01-14/NASA-01-7). Savoy, IL: University of Illinois, Aviation Research Lab.
- Wickens, C. D., & McCarley, J. S. (2001). Attention-situation awareness (A-SA) model of pilot error (Final Technical Report ARL-01-13/NASA-01-6). Savoy, IL: University of Illinois, Aviation Research Lab.

Appendix: Scatter plots from model version 2.

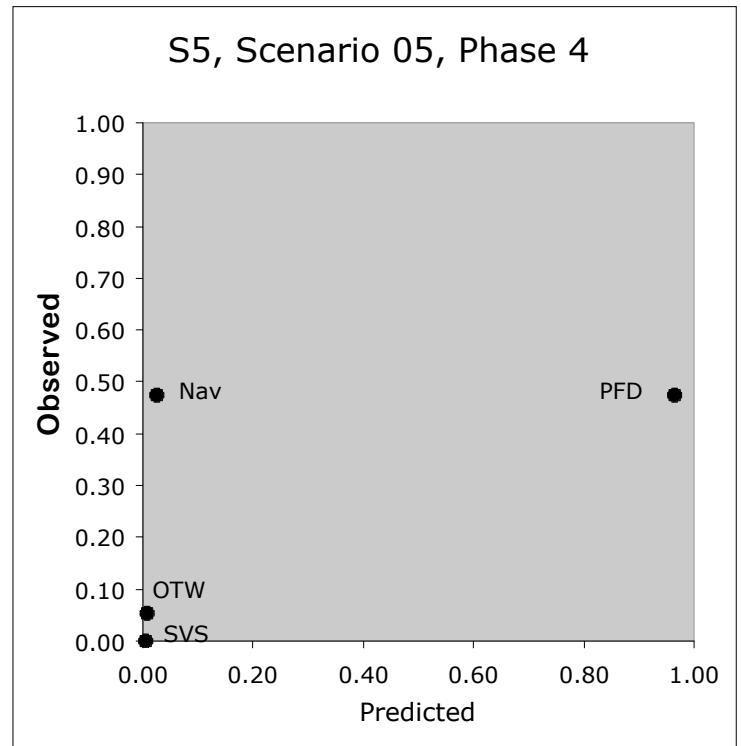
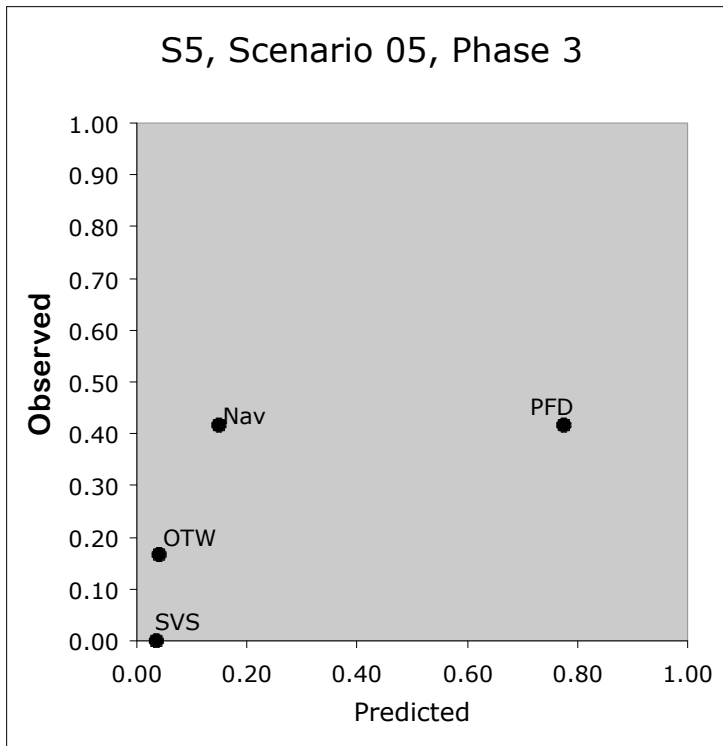
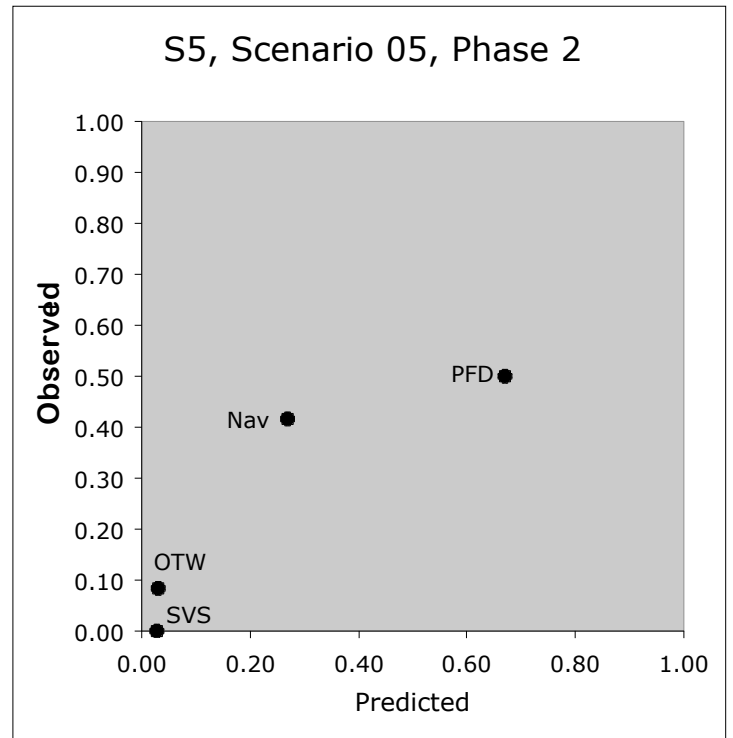
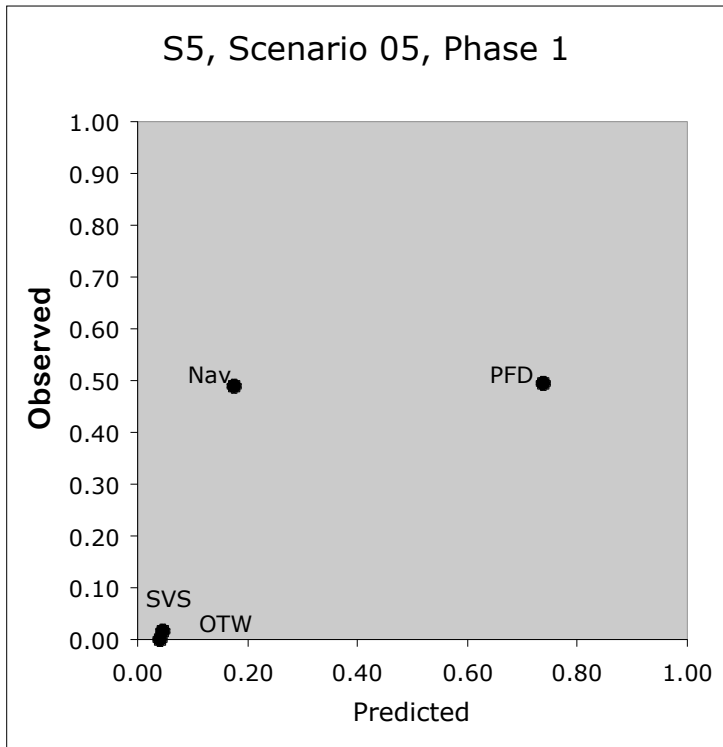
Scenario 5, Subject 3, Phases 1-4



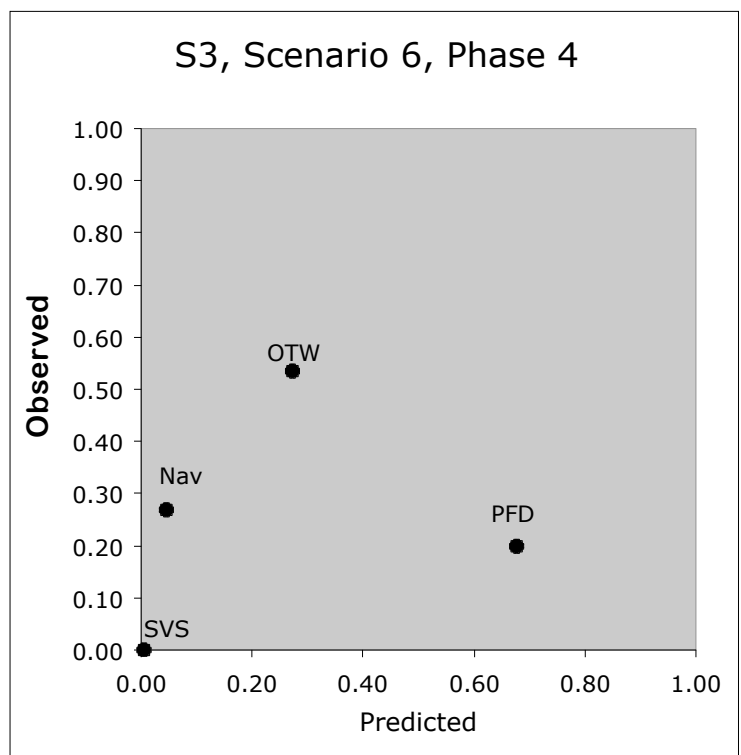
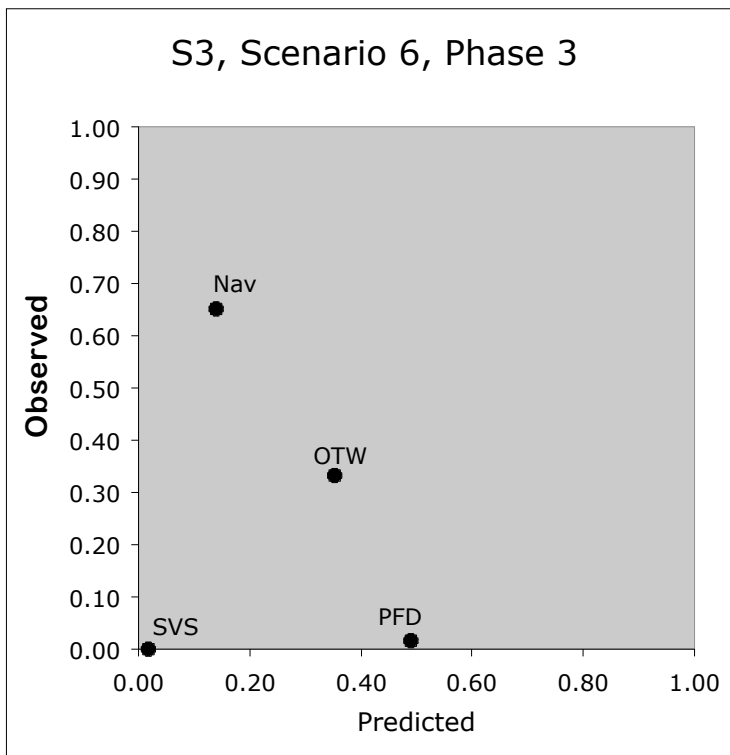
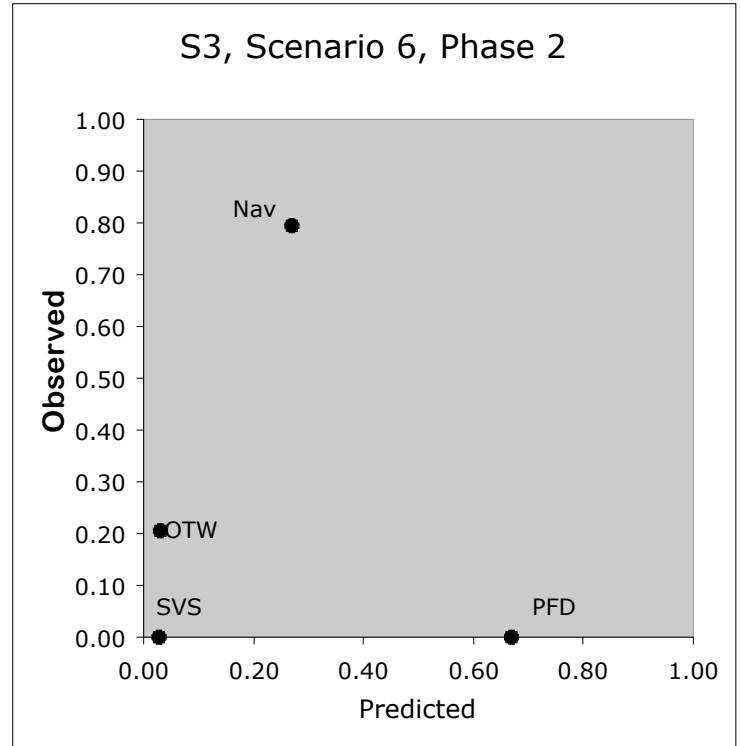
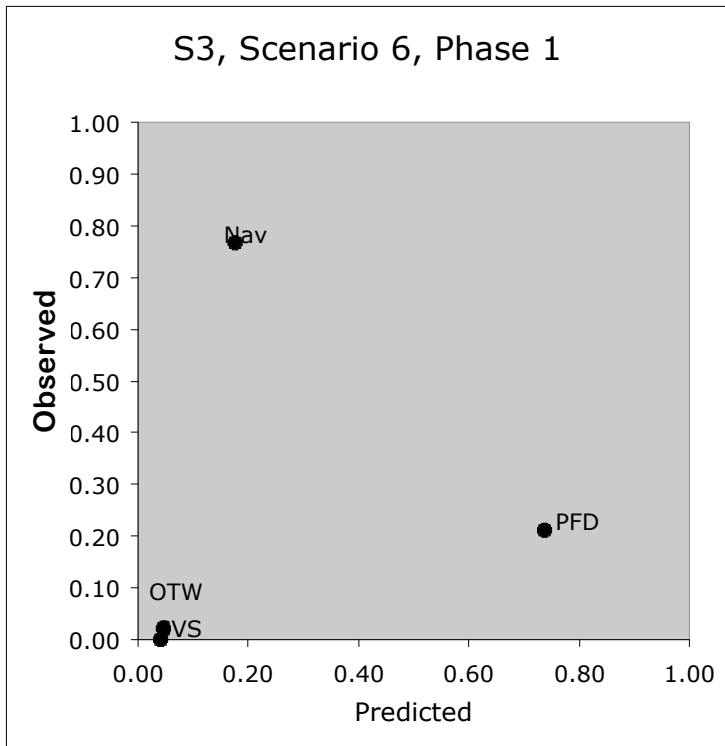
Scenario 5, Subject 4, Phases 1-4



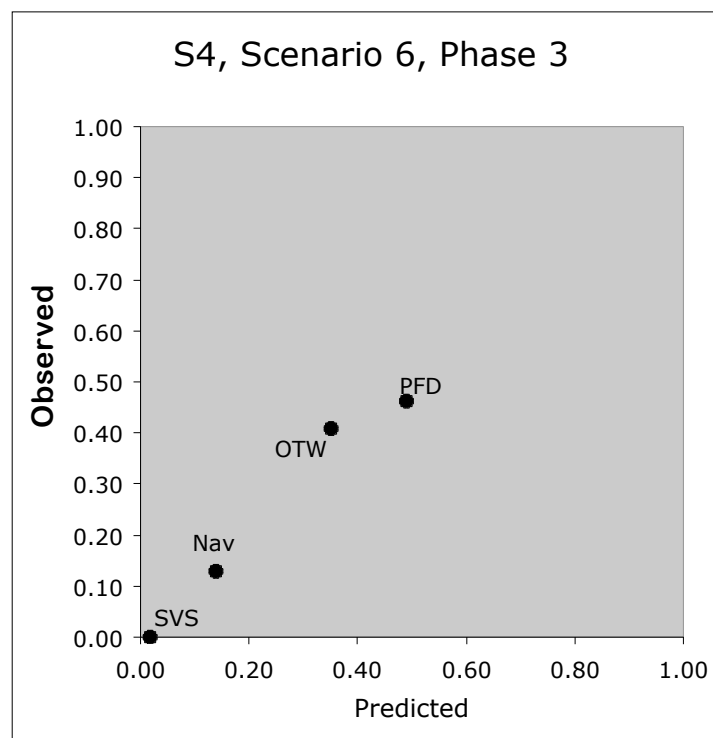
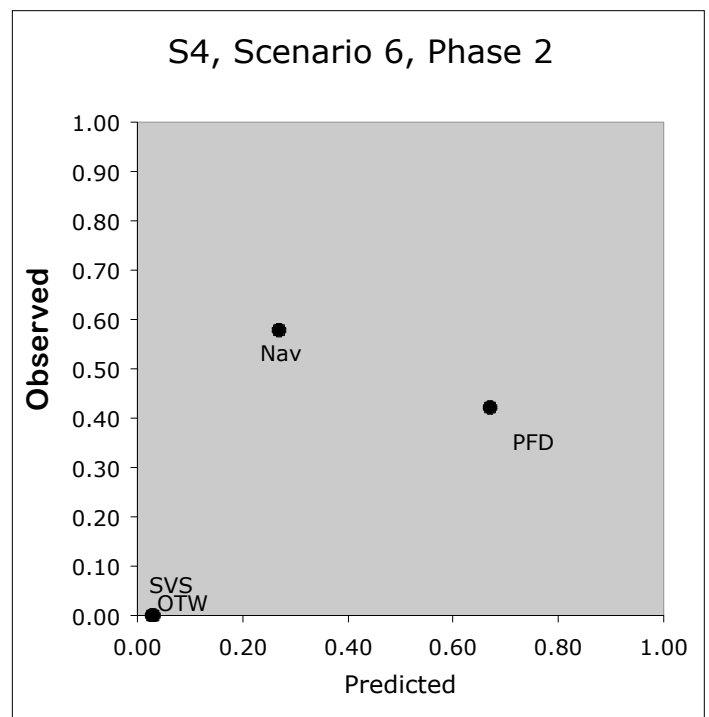
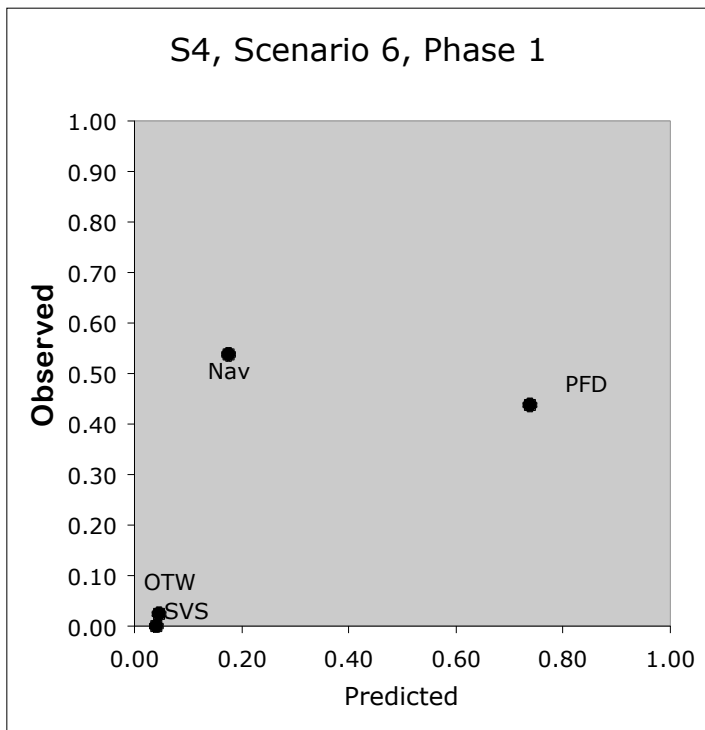
Scenario 5, Subject 5, Phases 1-4



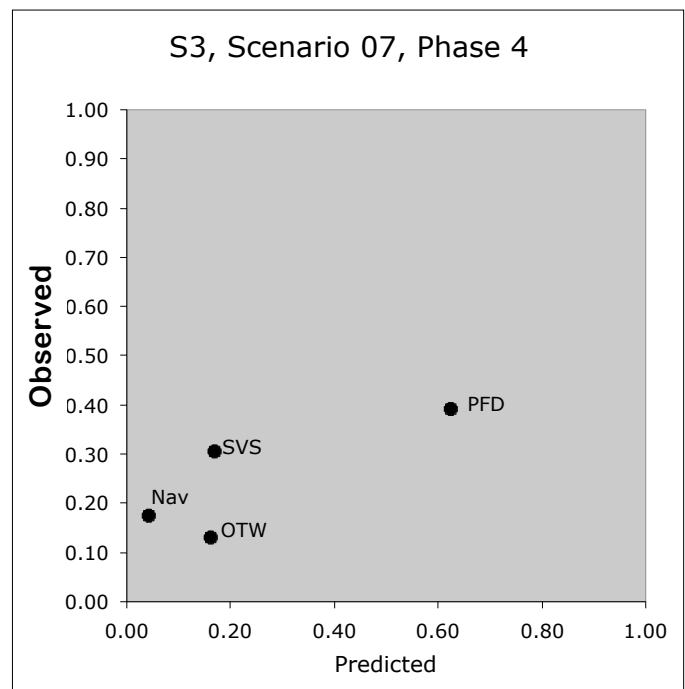
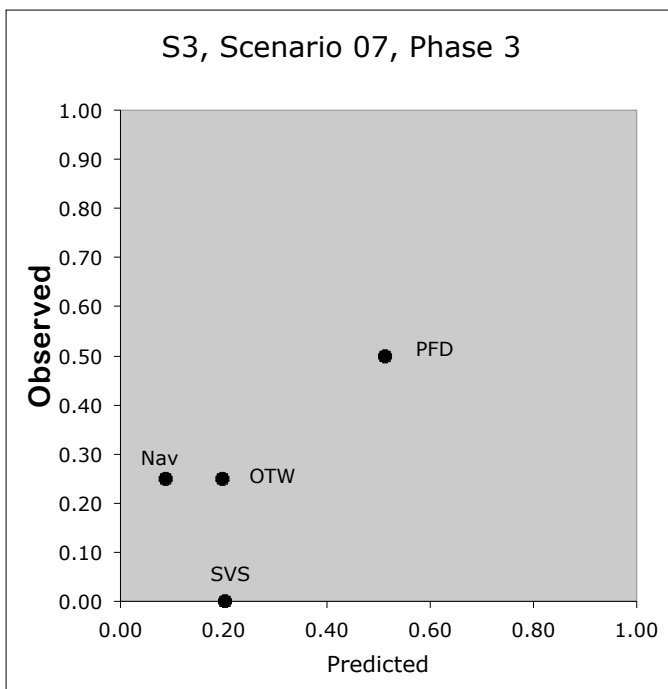
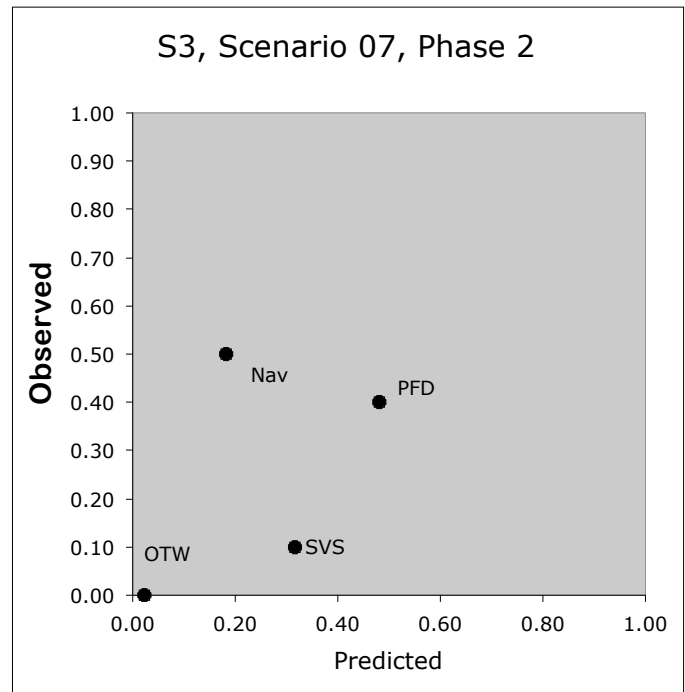
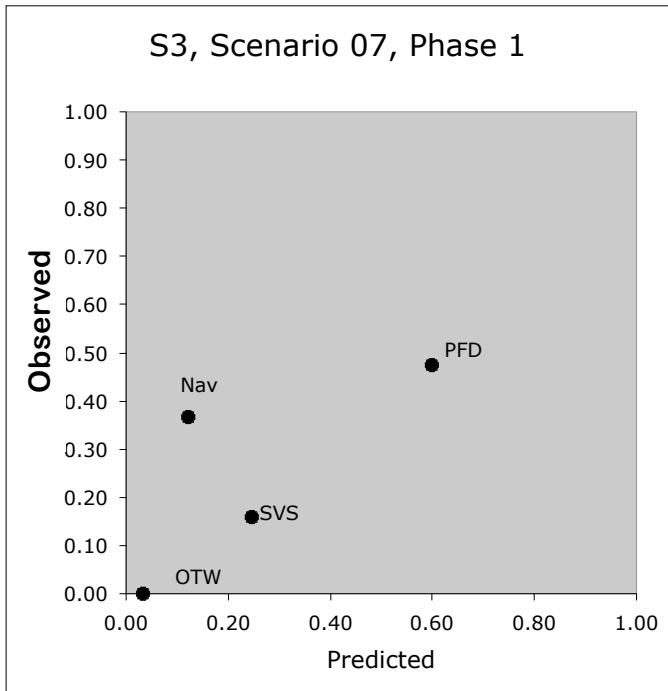
Scenario 6, Subject 3, Phases 1-4



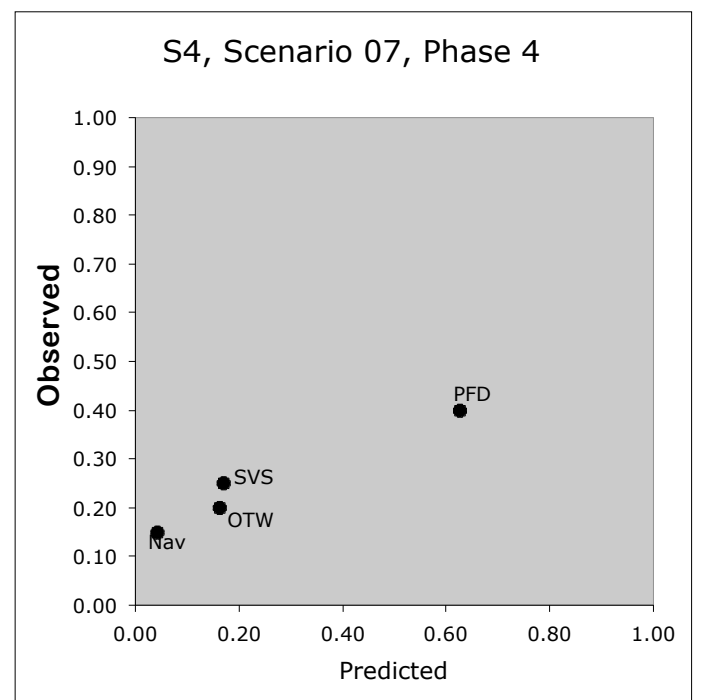
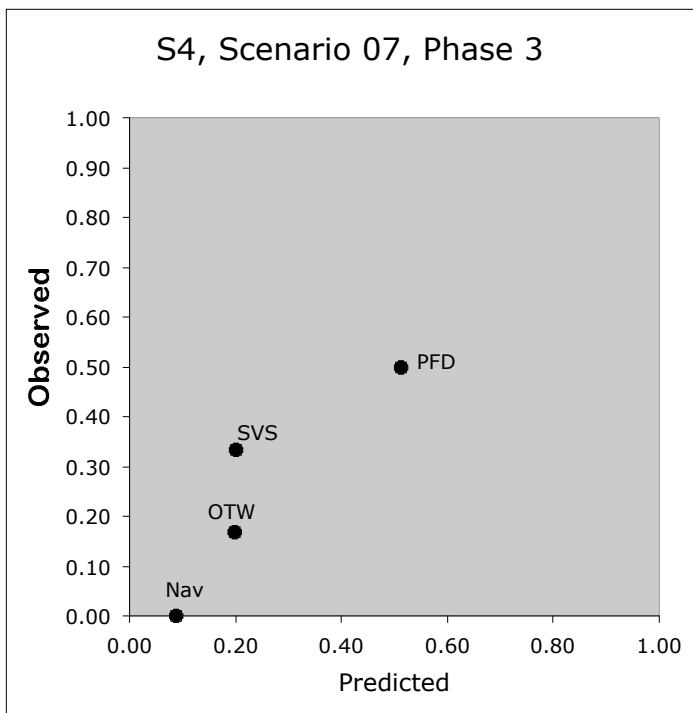
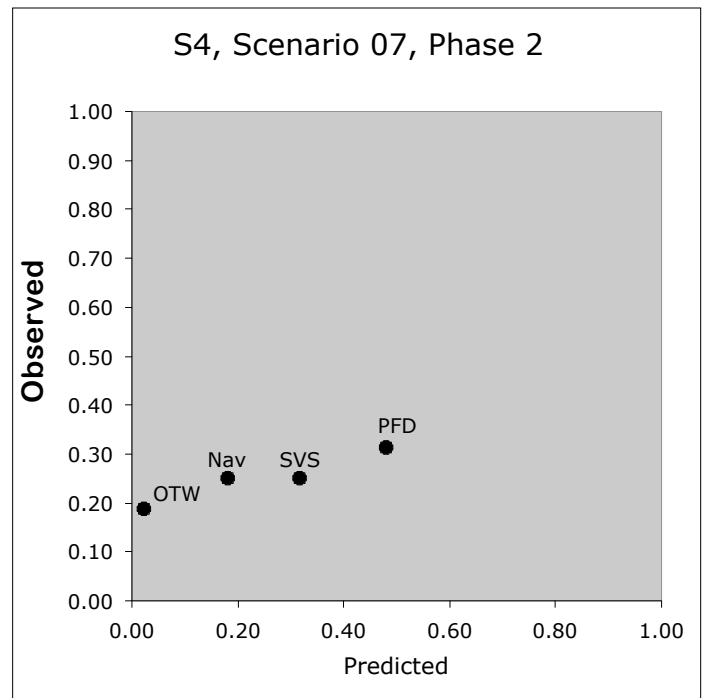
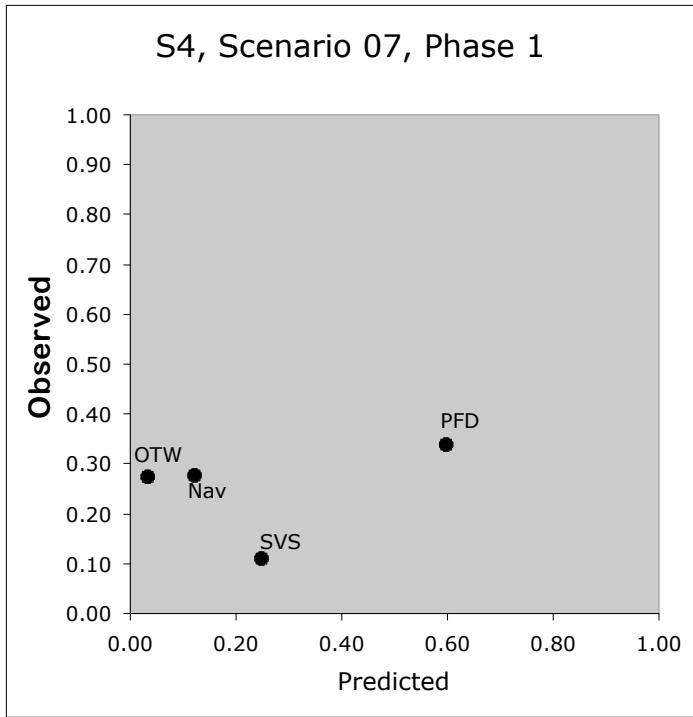
Scenario 6, Subject 4, Phases 1-3



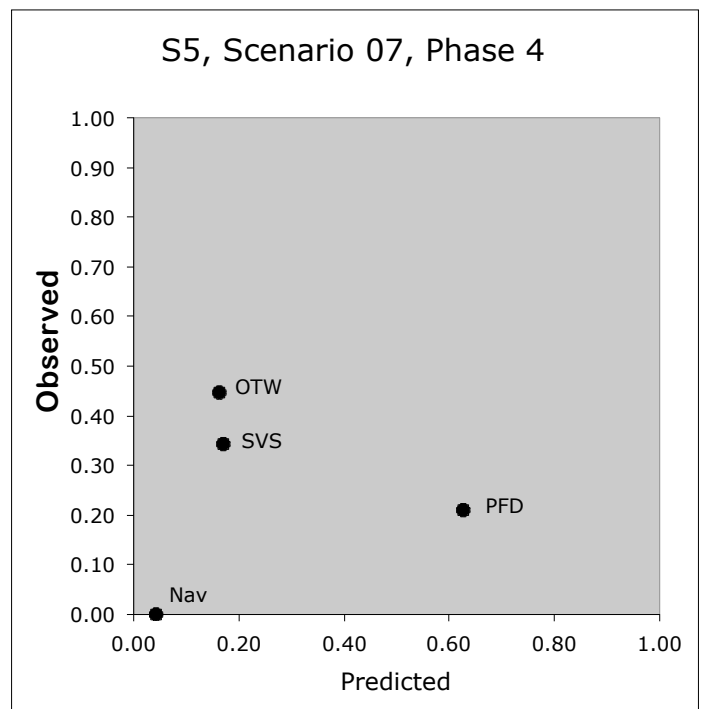
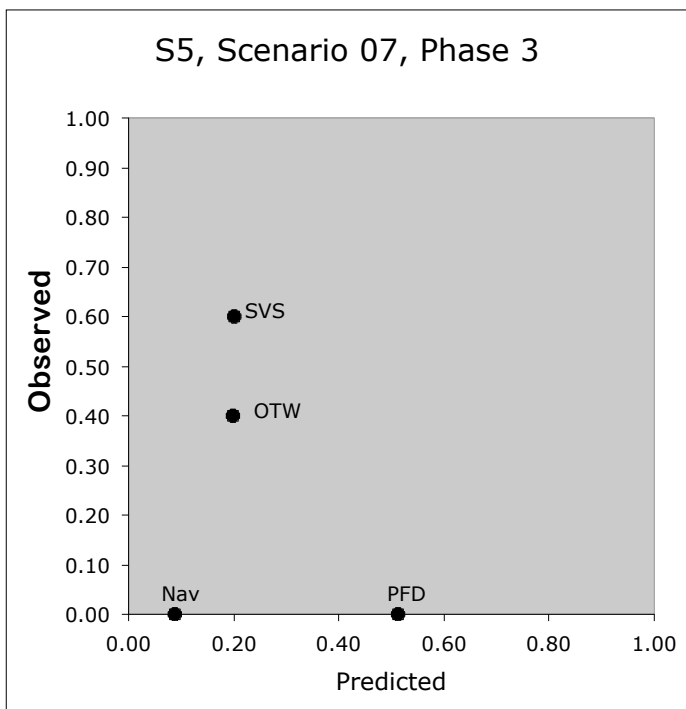
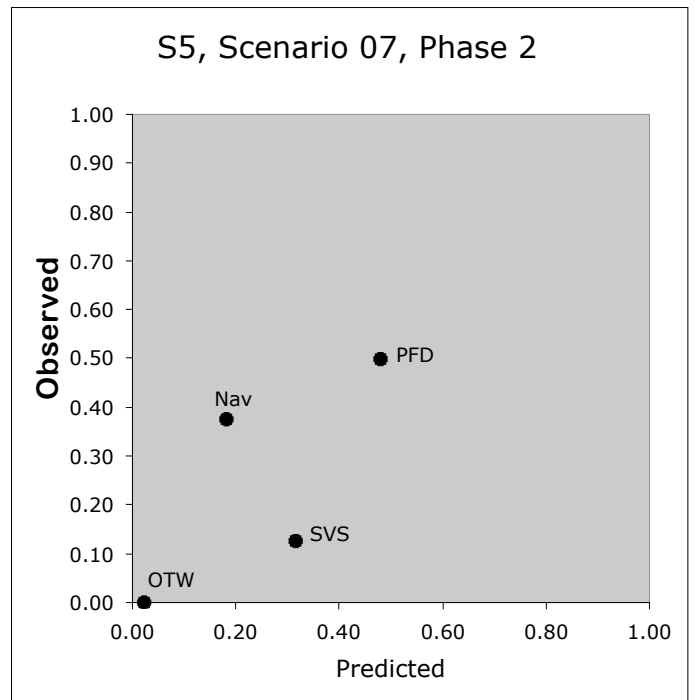
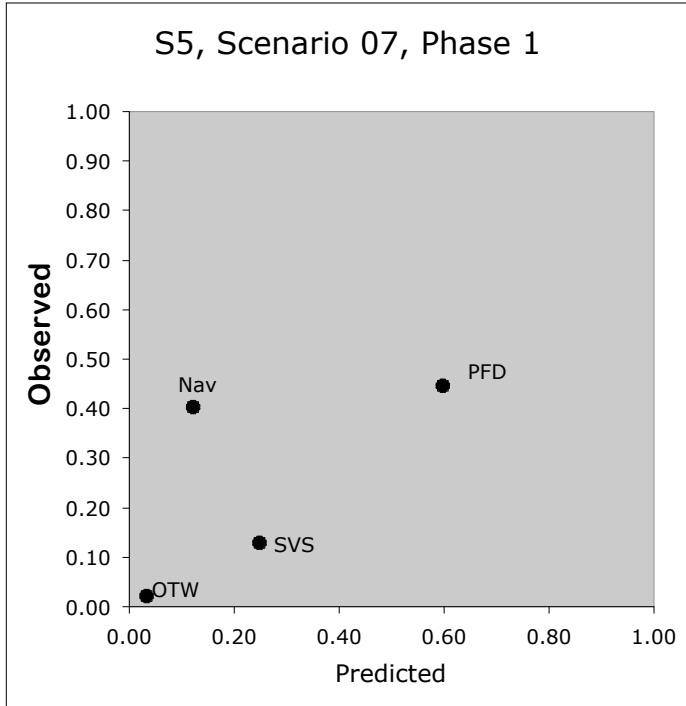
Scenario 7, Subject 3, Phases 1-4



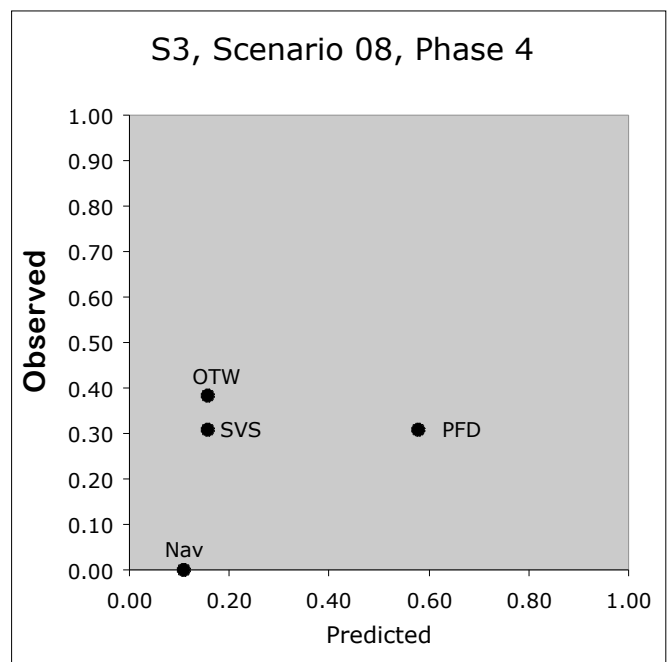
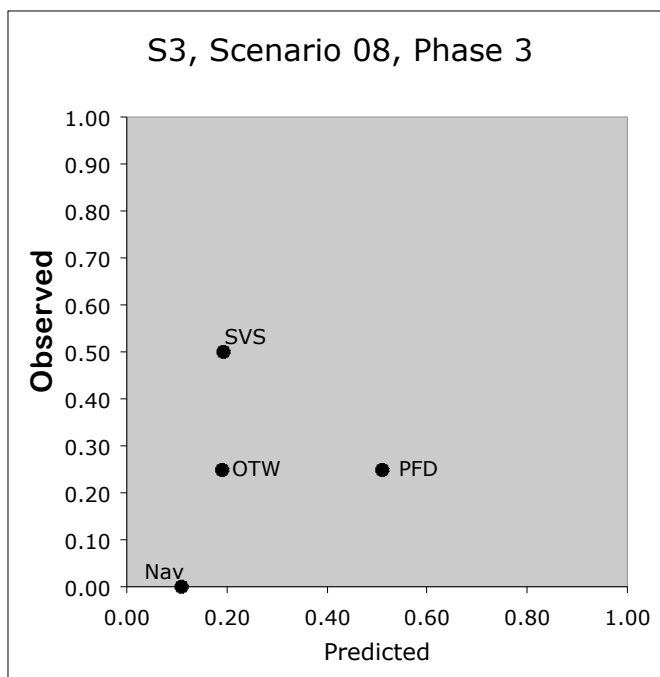
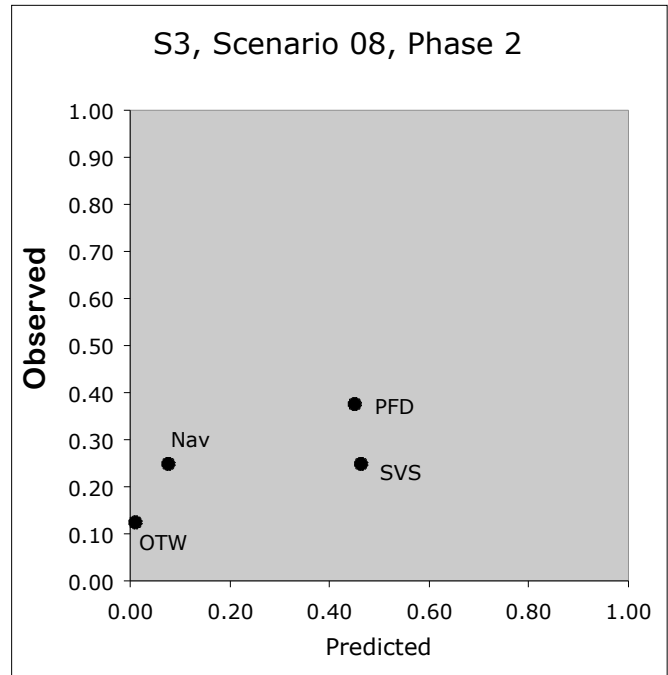
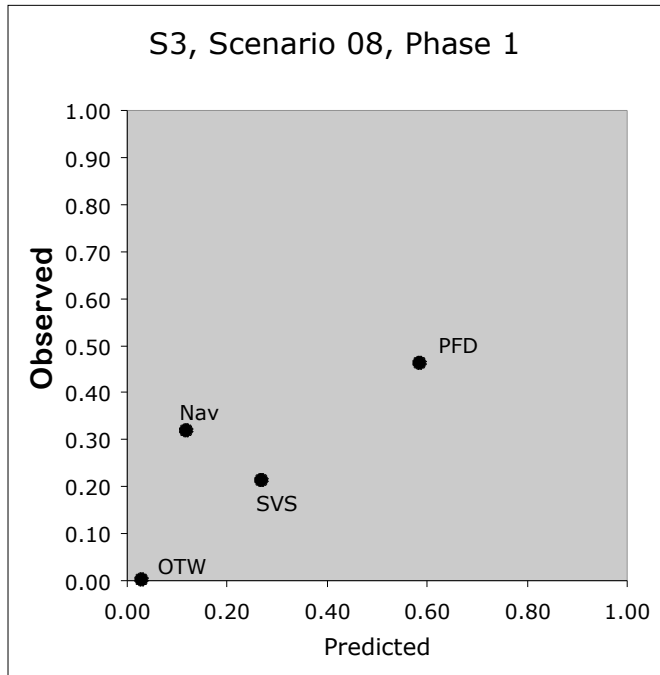
Scenario 7, Subject 4, Phases 1-4



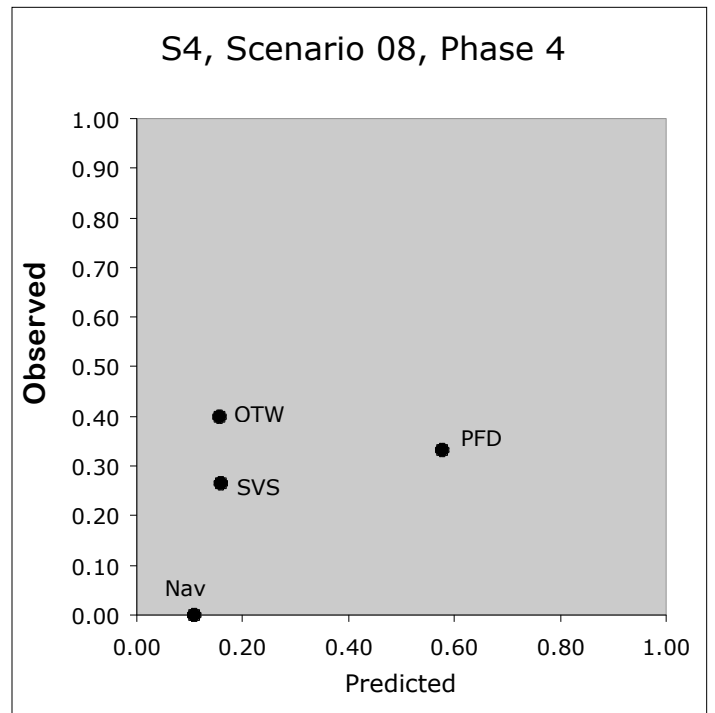
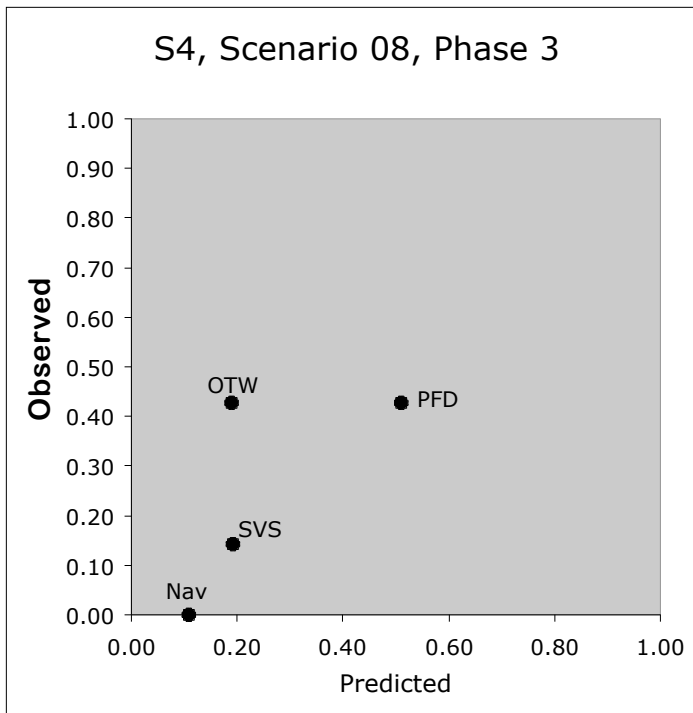
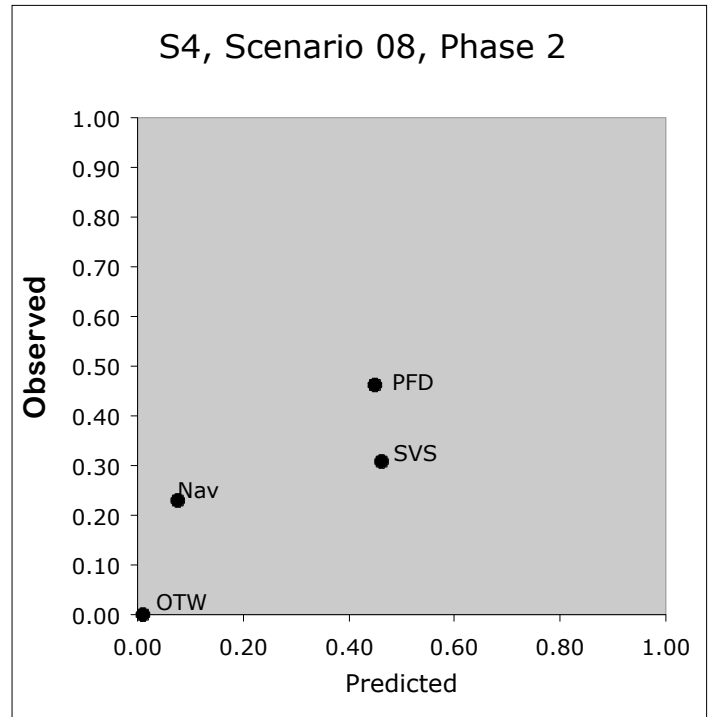
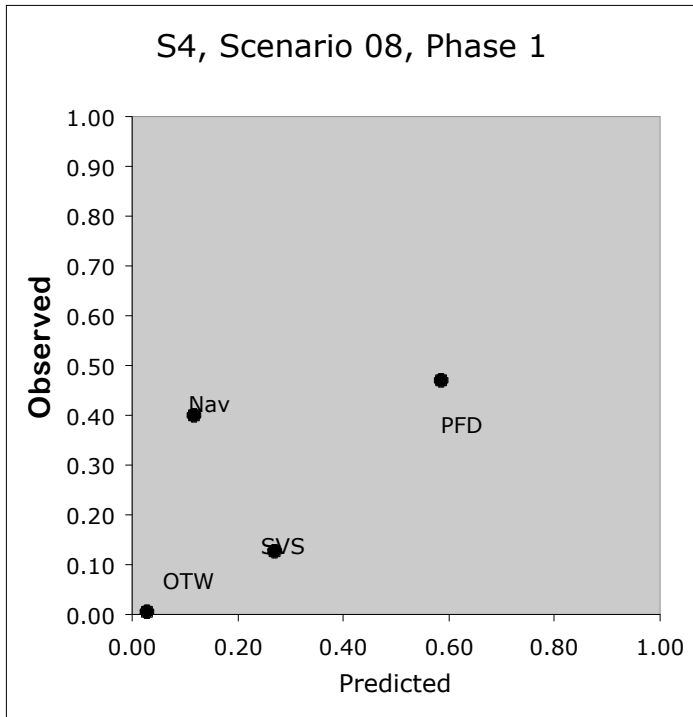
Scenario 7, Subject 5, Phases 1-4



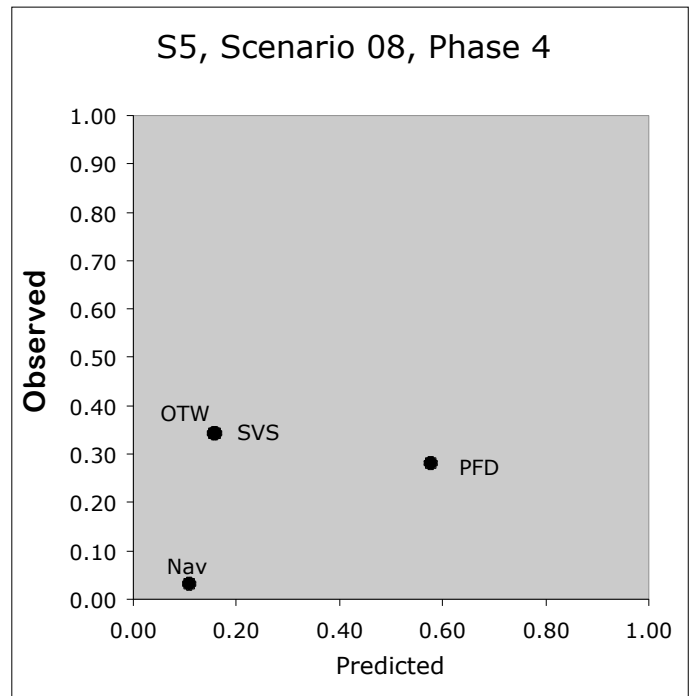
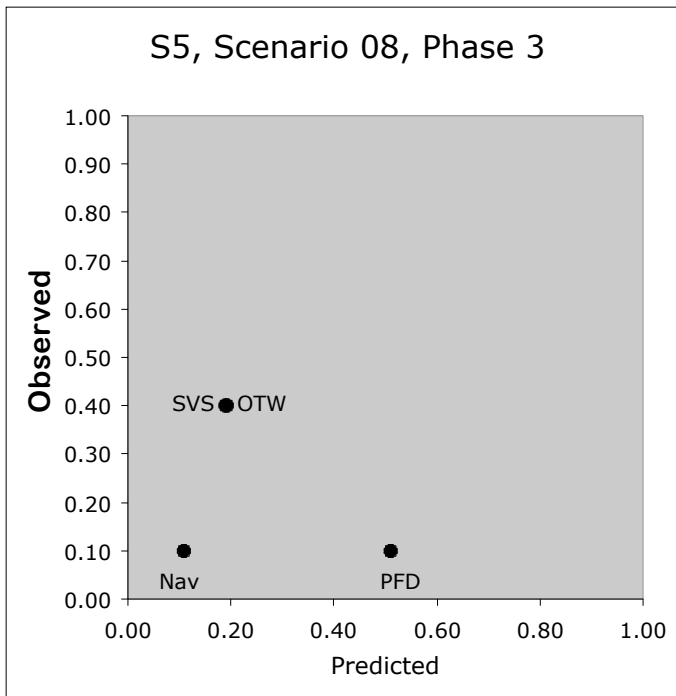
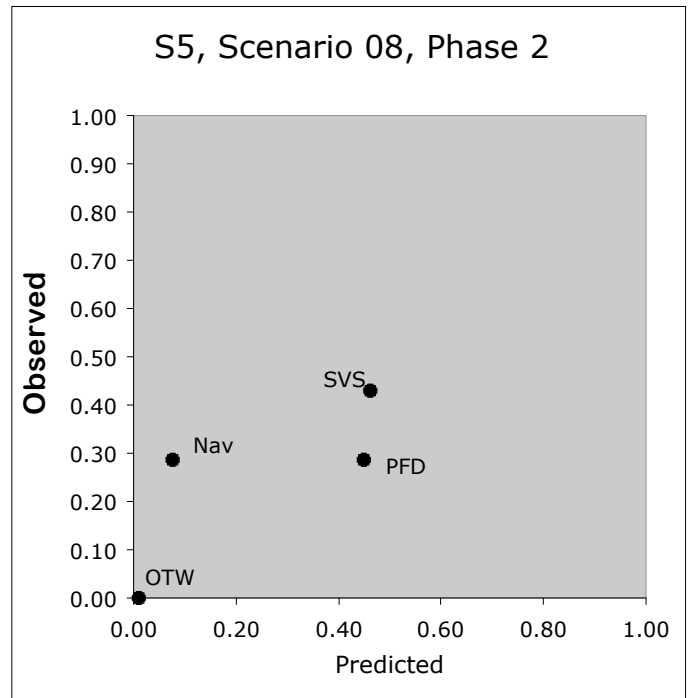
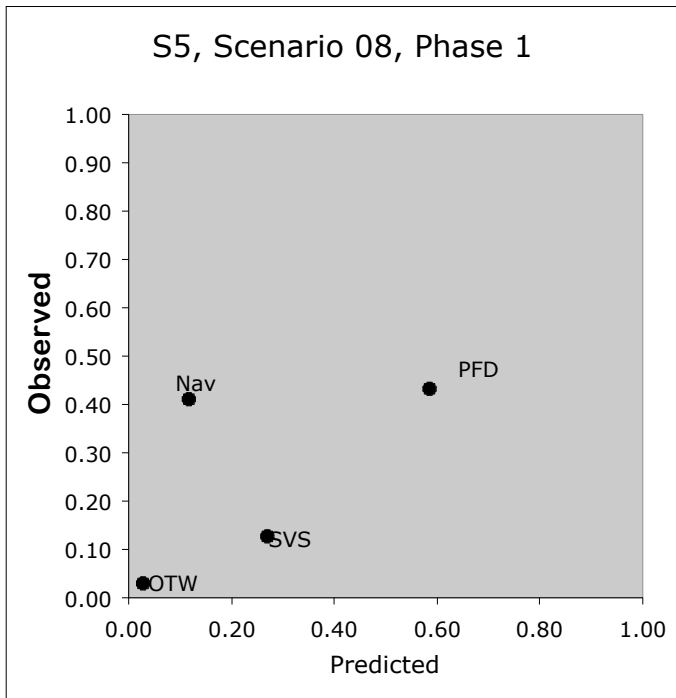
Scenario 8, Subject 3, Phases 1-4



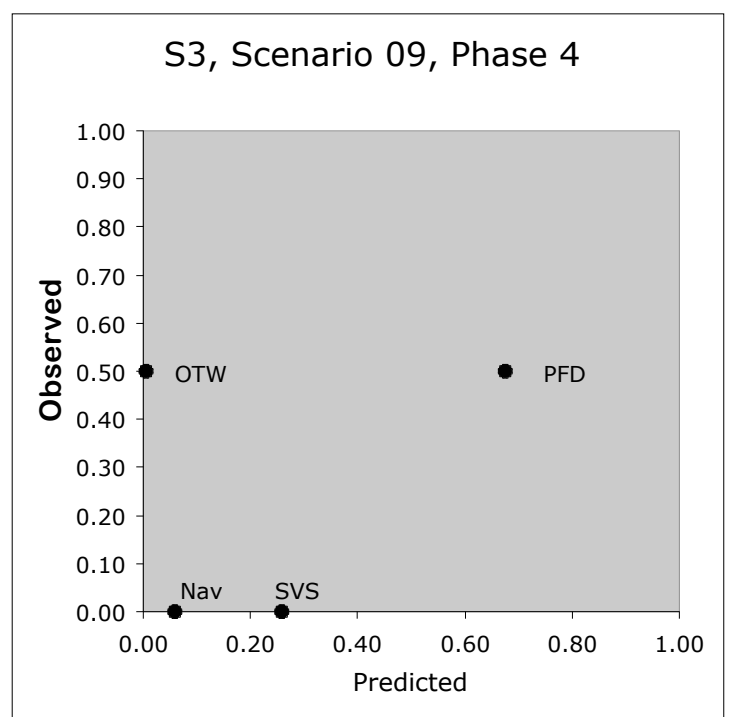
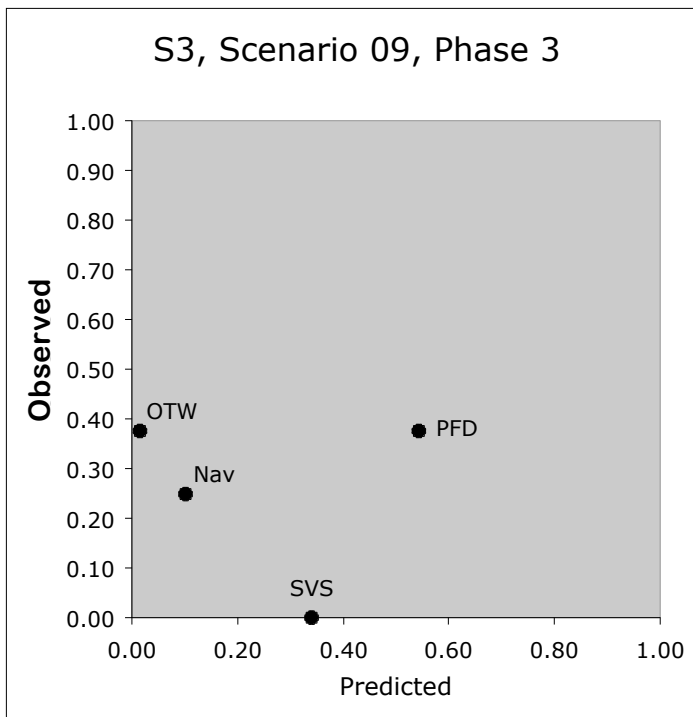
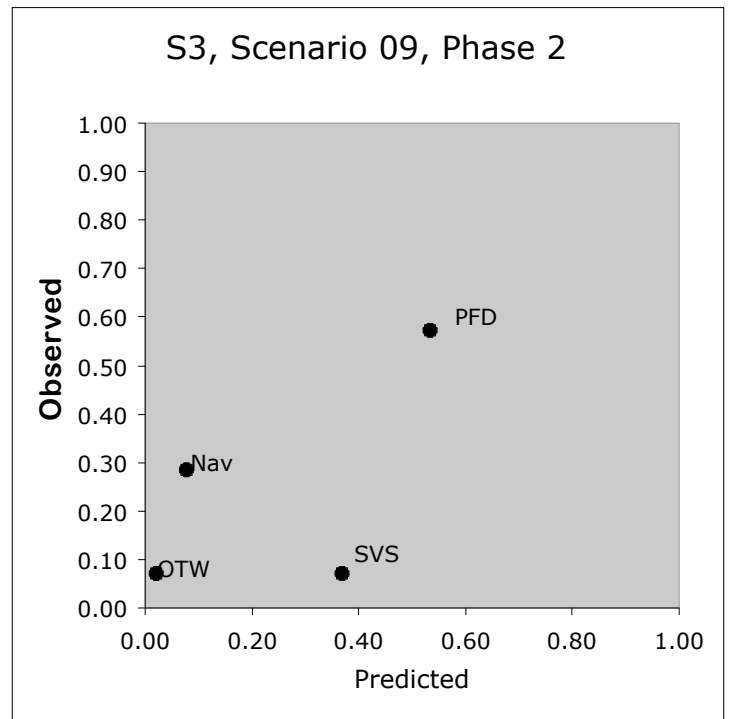
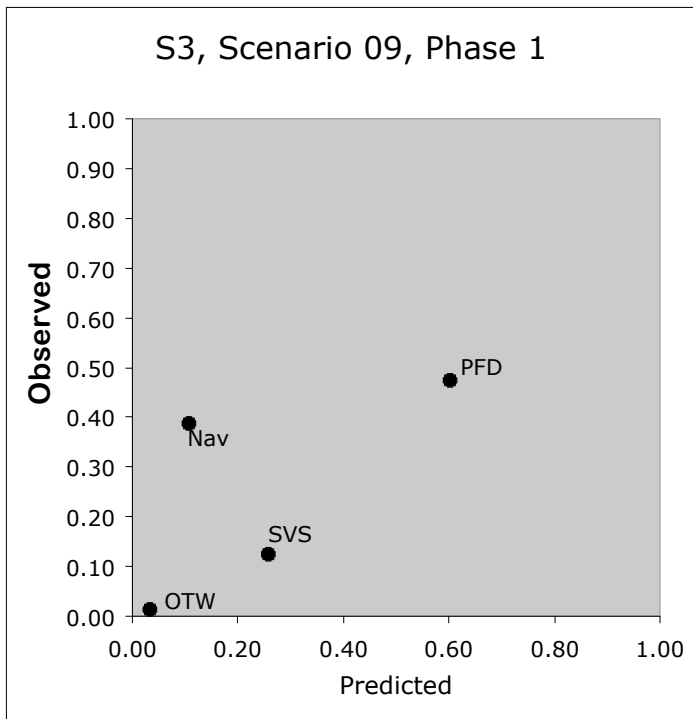
Scenario 8, Subject 4, Phases 1-4



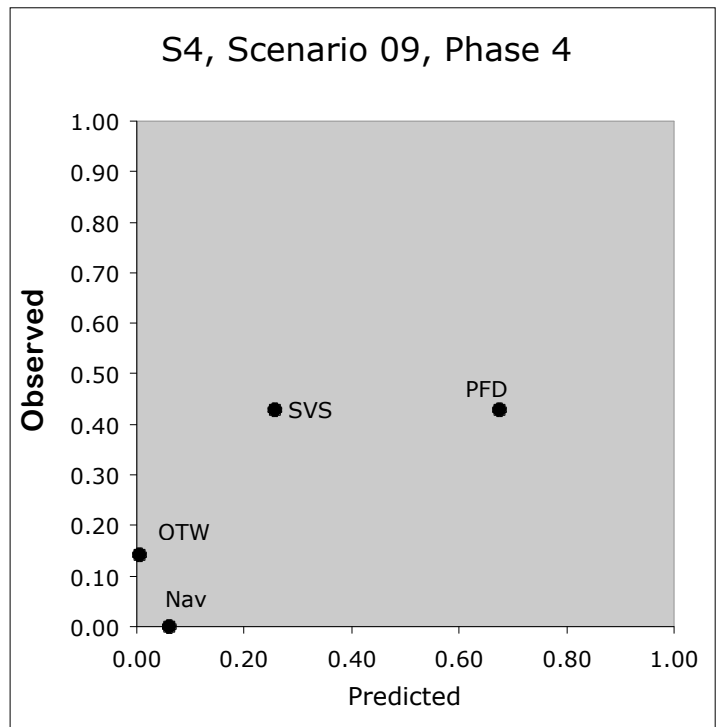
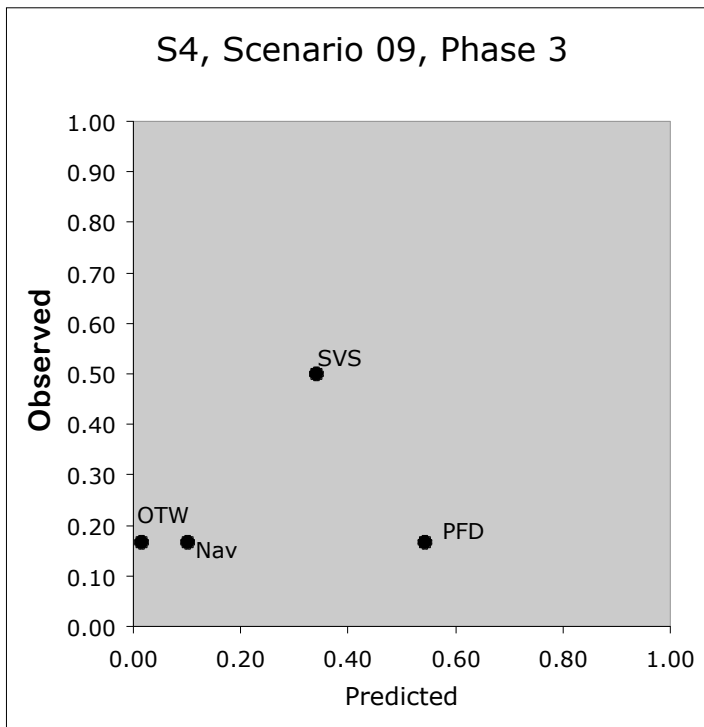
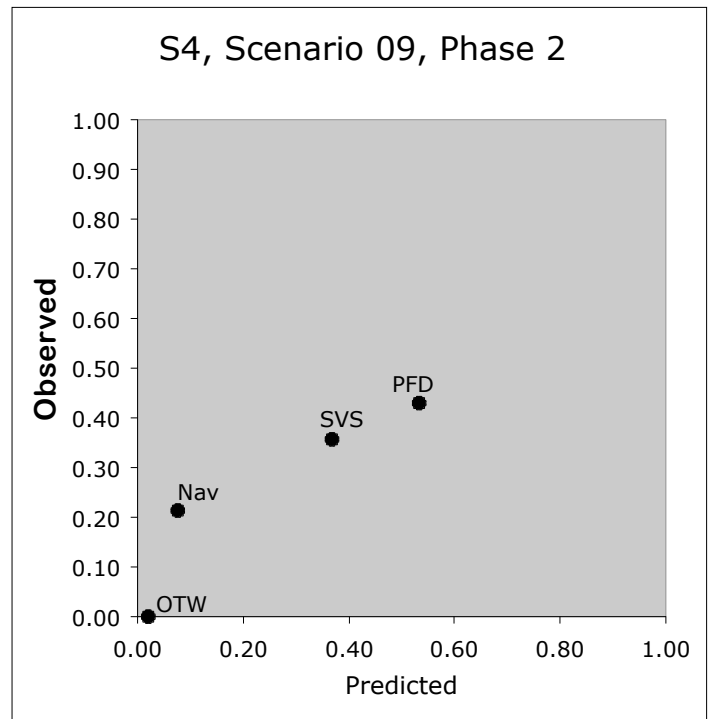
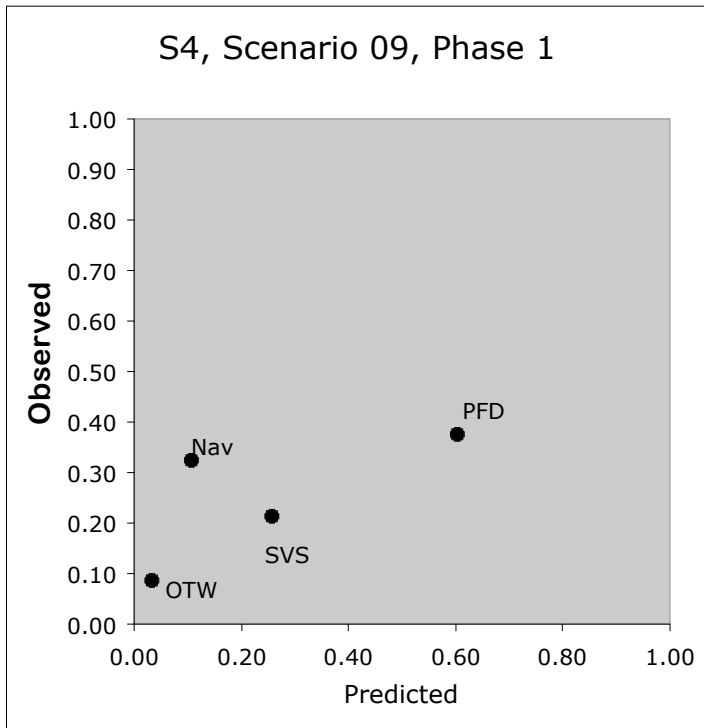
Scenario 8, Subject 5, Phases 1-4



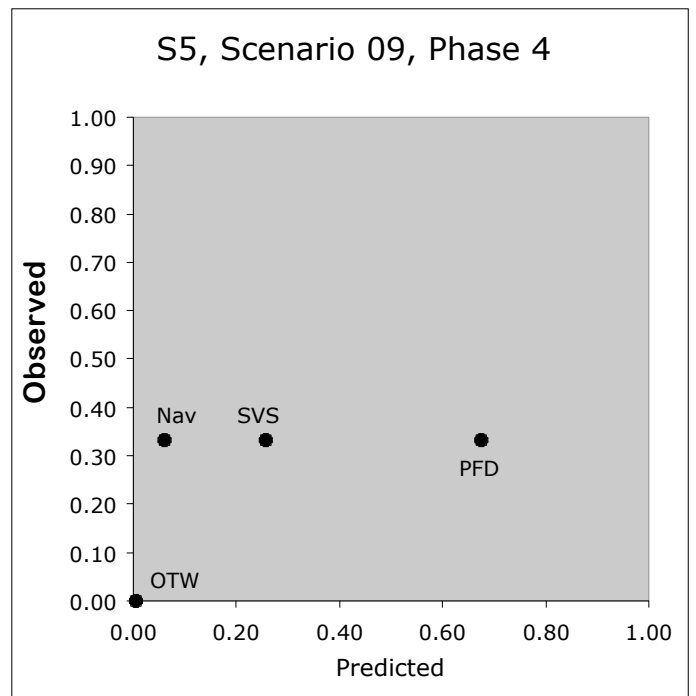
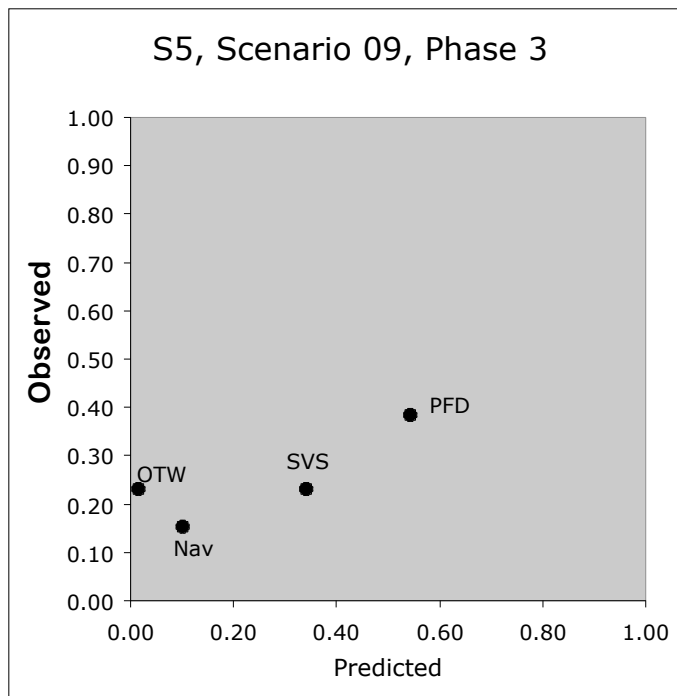
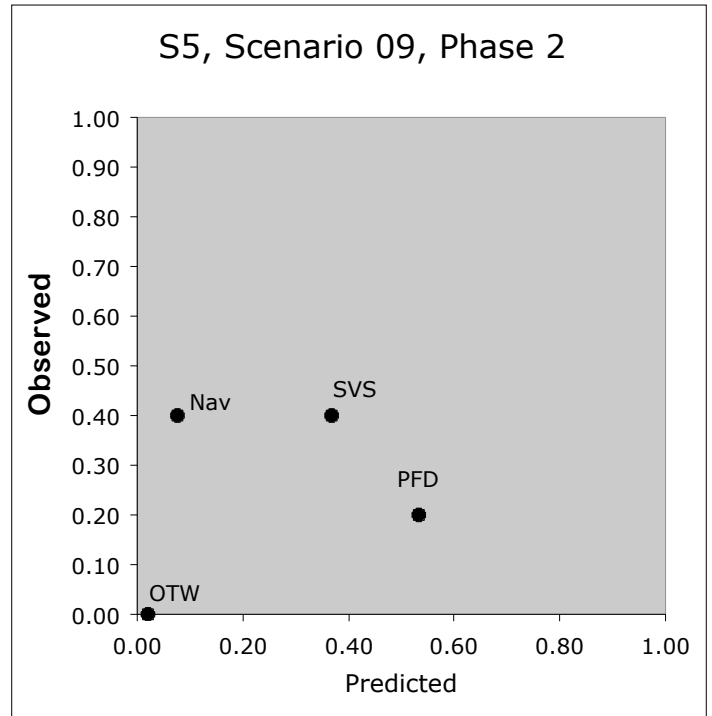
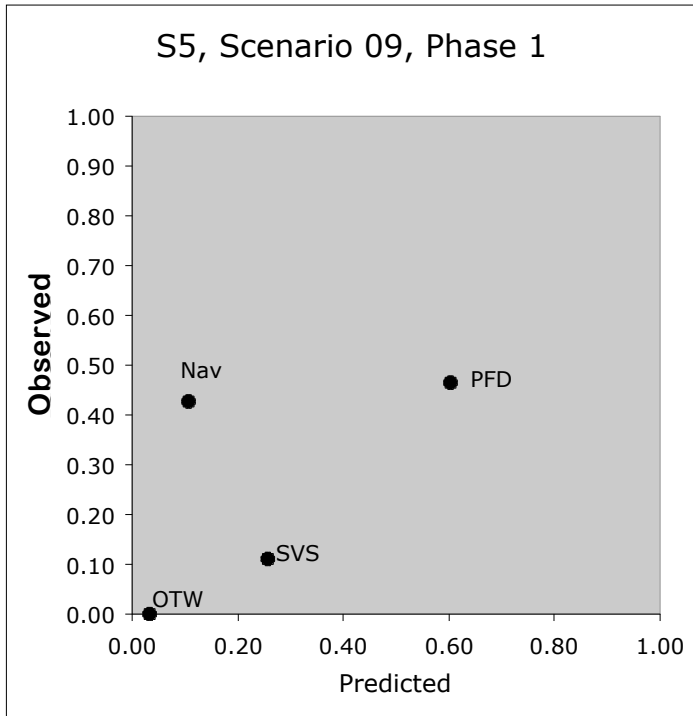
Scenario 9, Subject 3, Phases 1-4



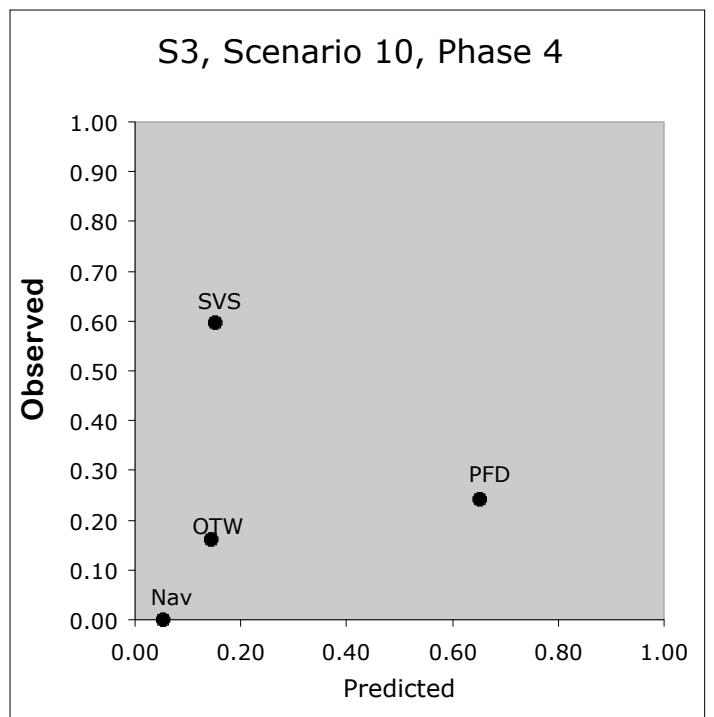
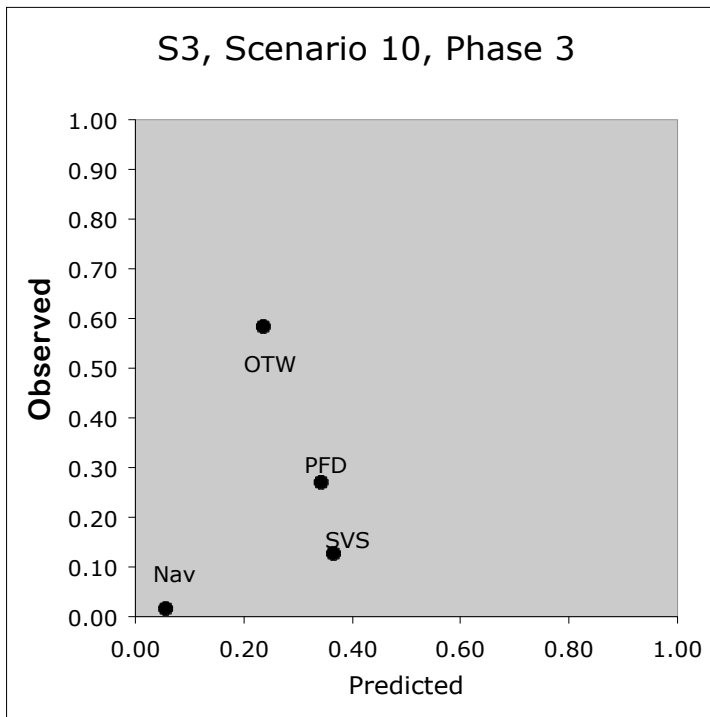
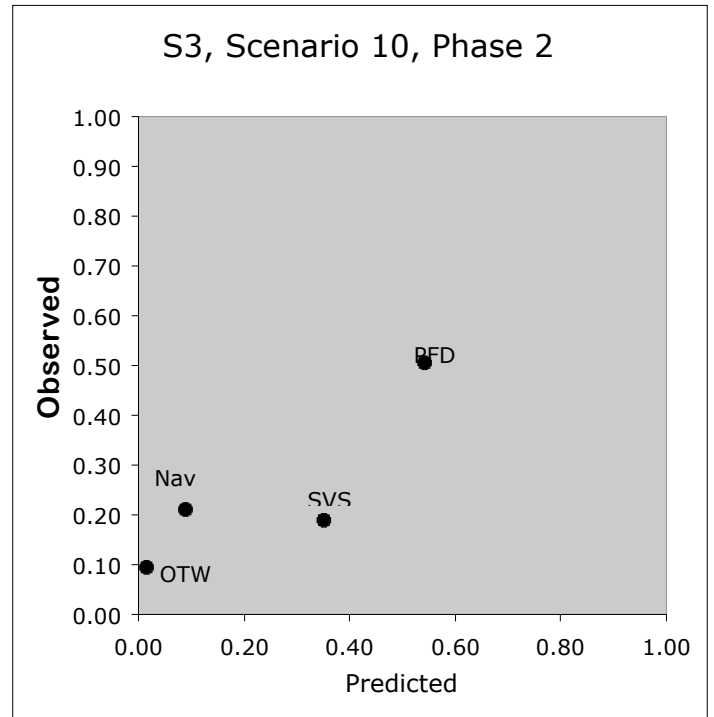
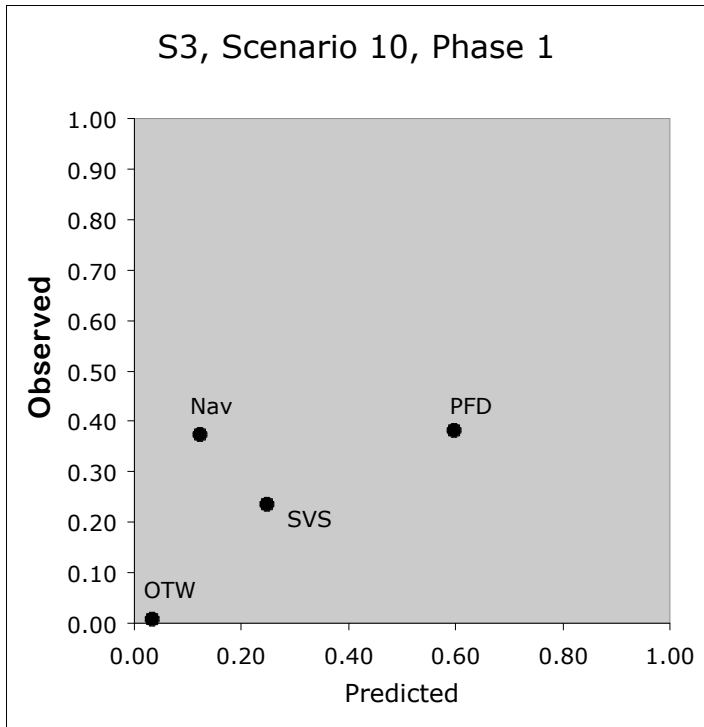
Scenario 9, Subject 4, Phases 1-4



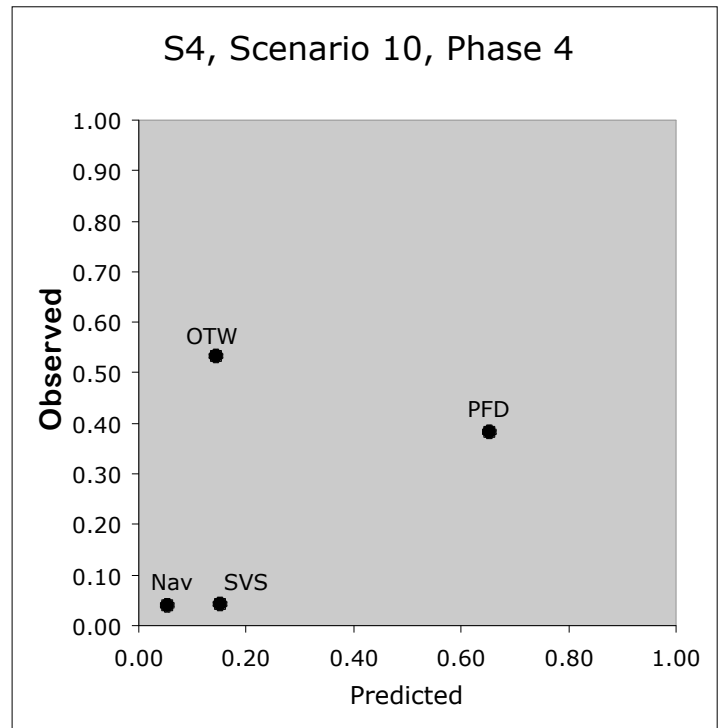
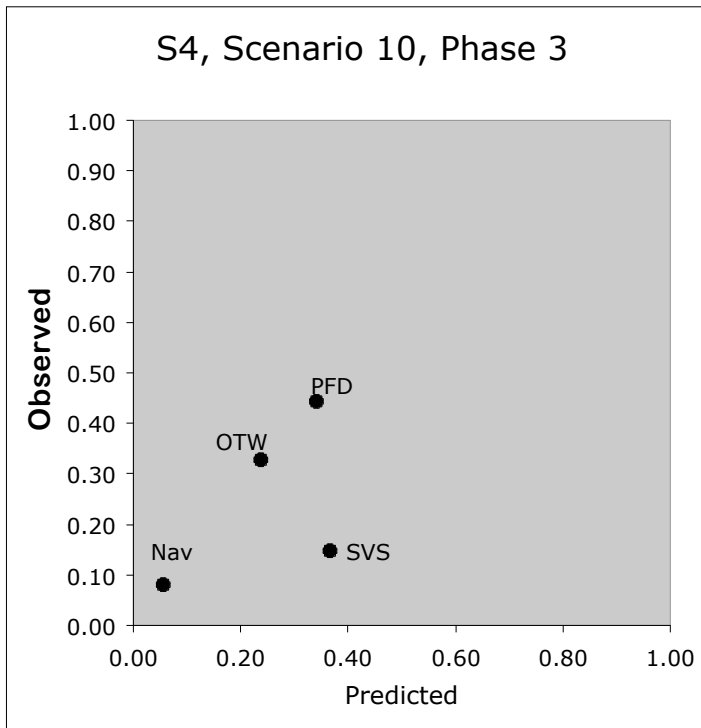
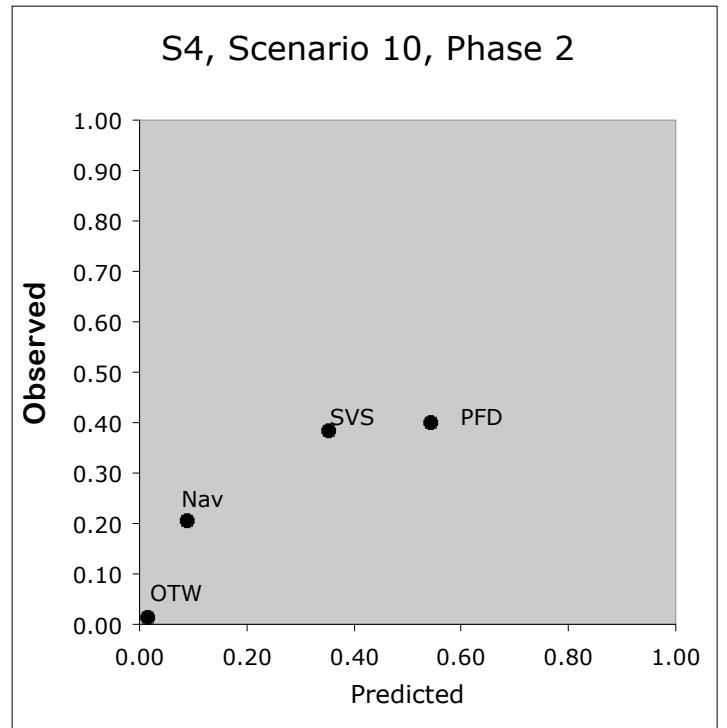
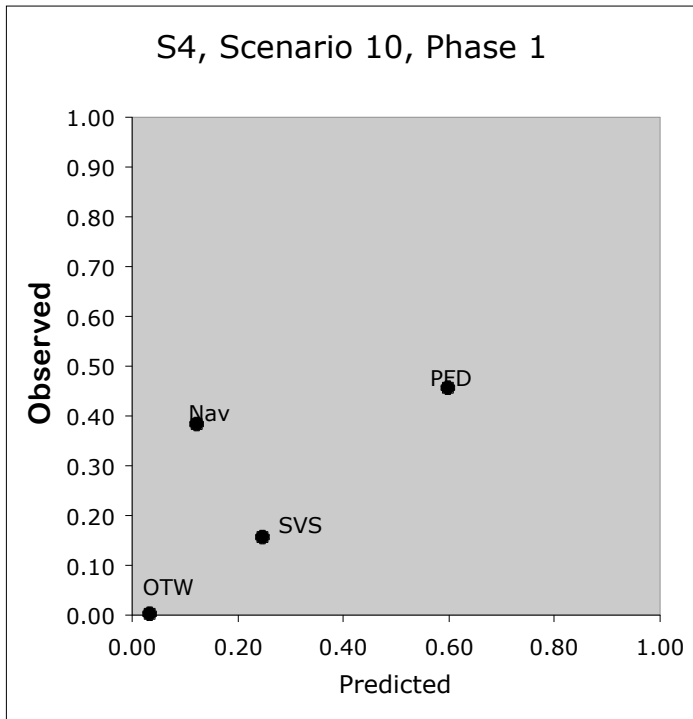
Scenario 9, Subject 5, Phases 1-4



Scenario 10, Subject 3, Phases 1-4



Scenario 10, Subject 4, Phases 1-4



Scenario 10, Subject 5, Phases 1-4

